



# D1.4 – Midterm Report, LOWCOST-IC

## PROJECT INFORMATION

<b>GRANT AGREEMENT NUMBER</b>	826323
<b>PROJECT FULL TITLE</b>	Low Cost Interconnects with highly improved Contact Strength for SOC Applications
<b>PROJECT ACRONYM</b>	LOWCOST-IC
<b>FUNDING SCHEME</b>	FCH-JU2
<b>START DATE OF THE PROJECT</b>	1/1-2019
<b>DURATION</b>	36 months
<b>CALL IDENTIFIER</b>	H2020-JTI-FCH-2018-1
<b>PROJECT WEBSITE</b>	www.lowcost-ic.eu

## DELIVERABLE INFORMATION

<b>WP NO.</b>	1
<b>WP LEADER</b>	Henrik Lund Frandsen
<b>CONTRIBUTING PARTNERS</b>	Aperam, AVL, Borit, Chalmers University, Forschungs Zentrum Jülich, Sandvik Material Technology, SOLIDpower, Sunfire, Technical University of Denmark, Techno Italia,
<b>NATURE</b>	Report
<b>AUTHORS</b>	Henrik Lund Frandsen, Karin Vels Hansen, Ragnar Kiebach, Pierre-Olivier Santacreu, Gert Nelissen, Carlos Bernuy-López, Dario Montinaro, Fabrizio Gualandris, Christian Walter, Martin Pötschke, Dino Boccaccini
<b>CONTRACTUAL DEADLINE</b>	31-06-2020
<b>DELIVERY DATE TO EC</b>	31-08-2020

## DISSEMINATION LEVEL

PU	Public	X
PP	Restricted to other programme participants (incl. Commission Services)	
RE	Restricted to a group specified by the consortium (incl. Commission Services)	
CO	Confidential, only for the members of the consortium (incl. Commission Services)	



## **1 Explanation of the work carried out by the beneficiaries and Overview of the progress**

The LOWCOST-IC project has the objectives of increasing the robustness of solid oxide fuel cell stacks while decreasing the cost of the interconnects. It brings together a consortium covering the entire value chain from the interconnect production to their final use in solid oxide cell stacks. To achieve the goals, a novel production route is tested together with a number of proposed material and analysis improvements.

In the first part of the project the focus has been on testing the feasibility of the new proposed materials in the laboratory, testing of new processing methods and setting up analysis tools. To ensure that all processes in the value chains can be used with the new materials, existing materials have been tested with the new processing methods to mitigate possible problems at an early stage. But also stack tests closer to the real use are performed to test the currently available materials.

One of the new materials used in the project is a pre-coated chromium rich ferritic steel from Sandvik (SAN), Sanergy® HT 441. The thin coating is deposited by physical vapour deposition (PVD). It was investigated whether the coating sustained the chosen hydroforming method conducted by Borit (BOR). No change of corrosion protection could be observed by Chalmers University (CU) after the shaping. It could thus be concluded that the cost-effective roll-to-roll production route, with PVD coating and hydroforming - proposed in the project, is feasible.

With respect to processing, the hydroforming by BOR was shown to be able to easily reproduce Sunfire's (SUN) interconnect shape using a 0.3 mm steel plate, whereas some deviations on the curvatures were present when using a stiffer 0.5 mm steel plate. To mitigate this limitation to the degree of freedom in the design process, a novel shape of interconnect ribs has been proposed by Forschung Zentrum Jülich (FZJ).

Besides the standard materials from Sandvik also another steel substrate, K44M, from Aperam (APE) and different coating solutions are investigated. Comparing the different steels, it was concluded by CU that coated K44M and AISI 441 offered similar performance in the lab, as the far more costly state-of-the-art steel, Crofer 22 APU. A replacement of this would induce a significant steel cost reduction (> 80 % reduction).

To join the interconnect with the ceramic cells, a so-called contact layer is needed, and the interface here is critical, as loss of contact will lead to failure of the stack. Here two novel contact layer materials from Technical University of Denmark (DTU) showed a very good performance in terms of high robustness (>200 % tough) and low area specific resistance (~15 mOhm.cm<sup>2</sup>). The chemical stability is better for the less robust (still very tough) contact layer and vice versa for the more robust contact layer, opening for the opportunity for further optimization by combining the two.



It was shown that the very fast drop on demand printing technology (40 m/min) could be used to print ceramic inks on the interconnect tops by Techno Italia (TI). This will save both material and make fast large-scale production feasible.

For the interconnect design process, a new very fast multiphysics stack model, which includes the local failure at the interconnect / air electrode interface, was developed by DTU. This reduces the time for a single computation of all physics relevant for a full stack from at least 40 hours to 15 minutes, making iterative design studies feasible. The flow distribution in this was verified using a detailed flow simulation by FZJ. The fast multiphysics model will in the following be used to optimize the interconnect geometry. The cost analysis was initiated by AVL, with preliminary results showing that it is possible to reduce the cost below 5 € per interconnect with the different proposed changes to the processing and materials.

Stacks with Sanergy® HT 441 were produced with the existing interconnect shaping methods and tested. For high temperature operation (850°C) at SUN, it was shown that Sanergy 441 HT corroded faster than the rather expensive Crofer 22 APU steel. The reason will be investigated in the second half of the project. The stack test of SOLIDpower's (SOL) stack at FZJ at 750°C are still ongoing.

## 1.1 Objectives

The project objectives are listed in Table 1 and the progress have been commented for each of these.

**Table 1. Status on Objective 1: Increasing the robustness and thus lifetime of the stacks**

#	Objective	Status
a)	Introducing contact layers based on a novel reactive oxidative bonding concept, which will increase the mechanical fracture energy of the cell-interconnect contact by > 200 % compared to state-of-the-art contact materials.	Achived. Novel contact layers with high mechanical robustness based on Co,Mn and Cu,Mn spinels have been achieved. Where the former shows better chemical stability, the latter shows exceptionally high mechanical robustness. New combinations will be explored.
b)	Applying highly protective coatings on both the air and the fuel side of the interconnect, thereby reducing the Ohmic resistance across the interconnect to < 15 mΩcm <sup>2</sup> at 750°C and < 20 mΩcm <sup>2</sup> at 850°C (evaluated after 3,000 h). The combination of the protective coating and a robust contact layer will reduce ASR-degradation to < 5 mΩcm <sup>2</sup> per 10 thermal cycles.	Achieved with high likeliness. Where the 850°C ASR was measured to 15 mΩcm <sup>2</sup> then the 750°C was measured to 18 mΩcm <sup>2</sup> , both <i>including</i> the ASR of the contact component. Without contact component these ASR values will be lower, but the resistance measurement of the contact component was rather uncertain, and the precise interconnect ASR could not be determined.
c)	Developing novel interconnect designs that reduce the maximum stress by > 30 %	Not yet achieved. All tools for achieving this have been successfully established, i.e.



	in the cell interconnect interface, while maintaining a low pressure drop (< 30 mbar), by use of computationally highly efficient SOC stack models.	novel interconnect rib geometry, 3D multiphysics model including mechanical stresses. Next, these will be brought together for optimizing geometry.
d)	Demonstrating stable operation for > 3000 hours and 50 cycles with the new contact layers and coated interconnects in multiple 1 kW stacks.	Partially achieved. Stack tests have been run for 3000 hours, but thermal cycling of stacks with new contact layers have not been carried out at this point in the project.

**Table 2. Status on Objective 2: Minimizing the interconnect development and production costs**

#	Objective	Status
a)	Introducing cheaper high-volume steel grades that reduce the interconnect raw material cost by > 80 %. The interconnect performance and lifetime will be retained by applying cost-effective protective coatings.	Achieved. Coated AISI 441 and K44M perform approximately similar to the more costly specially designed Crofer 22 APU in terms of Cr evaporation and oxide layer growth.
b)	Demonstrating the feasibility of combining state-of-the-art large-scale roll-to-roll manufacturing methods for both interconnect coating and shaping, and a fast drop-on-demand (DoD) printing (40 m/min) technology for application of the contact layer. This will reduce the fabrication costs to < 5 € per unit of interconnect including coatings and contact materials for processing at 50 MW/year capacity.	Partially achieved. Sandvik PVD-coated interconnect plates were hydroformed, and the corrosion resistance was shown to be retained after hydroforming. DoD printing on interconnect tops have also been demonstrated. The first preliminary cost assessment shows that this will make the interconnect price drop below 5 € per unit. Deeper analysis will verify this.
c)	Demonstrating a flexible and cost-effective interconnect development route with design iteration cost < 10 % of SoA, by using computationally highly efficient SOC stack models (>x10 faster than conventional models) for designing and hydroforming for shaping the interconnect.	Partially achieved. Cheap hydroforming of commercial interconnects was demonstrated. A method for shaping interconnect ribs have been proposed and feasibility is being tested. Fast computational model of Sunfire stack has been developed.



## 1.2 Explanation of the work carried per WP

In the following an executive summary is provided for each of the work packages together with an overall description of the activities in each of the tasks.

### 1.2.1 WP 1 - Project Management

#### Executive summary of WP1

The overall objective of this work package is to provide high quality in project management to ensure that the objectives are fulfilled within budget, on time, while minimizing risks. And if challenges occur, to mitigate these with the least impact of the outcome of the project.

The deliverables of WP1 is listed in Table 3. All deliverables were delivered on time. The intranet (D1.3) was available since project start, but the description of it was handed in somewhat later.

**Table 3. Deliverables in WP1, lead partner, and delivery dates.**

Del No	Title	Lead	Original Date	Delivery date/ New date
D1.1	Test protocol established among consortium partners	DTU	M3	M3
D1.2	Data management plan	DTU	M3	M3
D1.3	Intranet for reporting and file sharing established	DTU	M6	M8
D1.4	Midterm report	DTU	M18	M20
D1.5	Final report	DTU	M36	M42
D1.6	Annual data reporting	DTU	M18	M18
D1.7	Annual data reporting 2	DTU	M30	M36
D1.8	Annual data reporting 3	DTU	M36	M36
D1.9	Updated communication plan	DTU	M12	M15

Guidelines for how data generated by the project will be handled, stored, shared and protected was established in a Data Management Plan (DMP) (D1.2).

The midterm report D1.4 was estimated to be finalized earlier than needed (M18), and to include as much as possible after the Corona lock downs, this will be handed in slightly later (M20).

To handle the limited possibility to work on the project during the Corona pandemic, the project coordinator has proposed an extension of the project of 6 months. This has been approved by the consortium. Thus, we propose that more or less all deliverables and milestones from the Corona pandemic appearance and onwards are moved 6 months ahead. For each work package there are tables giving an overview of the status of the deliverables and milestones. In these the original delivery dates are followed by a column with new proposed delivery dates according to the delay because of the Corona pandemic. If



deliverables have already been handed in, the same column provides the actual date that the deliverable have been reported on the participant portal.

The deliverables and milestones are written with:

- green if delivered on time / with a minor delay, which do not impact the project plan.
- yellow if it impacts the project plan without overall delays (described further in Section 5)
- red if the deliverable impacts the project plan and cannot be handled within the current planning (extensions are needed).

Minor delays have been present through the project execution and some more significant delays has occurred, but a plan for mitigating issues relating to this, within the timeline of the project, is outlined in Section 5, why they have all been coloured yellow. We have not coloured changes due to the Corona pandemic (as this would make everything from now on red and will not give a clear picture of the actual project status).

With an extension due to the Corona pandemic, it is believed that the project plan can be followed without need for further extensions. The main uncertainty in this planning is of course the Corona pandemic and a possible second wave.

### T1.1 Project management and financial management

The project lead partner, DTU, has called for regular meetings and facilitated interaction between the partners across the work packages.

DTU has also made project support available assisting the project coordinator with practical tasks such as setting up meetings, set-up and maintenance of the project website and intranet, monitoring of the progress and notification of deadlines for deliverables and milestones and preparing periodic financial reports and activity reports to the EC.

A steering board has been appointed at the kick-off meeting with a representative from each of the partners.

### T1.2 Project progress and steering board meetings

Four project meetings have been held including the kick-off meeting. Three of these have been physical meetings and the fourth was held online, due to the Corona pandemic. Besides, a number of follow up meetings have been held by phone or online to ensure a continuous progress in the project. These have been listed in Table 4.

**Table 4. List of meetings for the entire consortium.**

Date	Meeting type	Location
22-23/1 2019	Kick-off meeting	Roskilde, Denmark DTU Risø Campus
15/5 2019	Telecon follow up meeting	Phone
11/9 2019	1st project meeting	Kyoto, Japan SOFC XVI Conference
13/11 2019	Telecon follow up meeting	Phone



5-6/2	2020	2nd project meeting	Geel, Belgium Borit NV
13/5	2020	Online follow up meeting	Microsoft Teams
4/6	2020	3rd project meeting, online	Zoom

Steering board meetings have been held after each of the four project meetings.

### T1.3 Coordinate test protocols

Two meetings have been held to coordinate the test-protocols. One in connection with the kick-off meeting and a second online meeting. This resulted in the written test protocol D1.1 unifying the lab test and closer to real application stack test for consistent and comparable results.

## 1.2.2 WP2 - Evaluation and manufacturing of steel grades and coatings

### Executive summary of WP2

The overall goal of WP2 is to explore and evaluate steel grades, coatings, and manufacturing processes to reduce the overall cost of the interconnects without affecting the performance. This is achieved by identifying the best high-volume steel grades and highly protective coating combinations for the SOC operating conditions. This steel-coating combination must demonstrate the feasibility to manufacture with a high-volume roll-to-roll manufacturing process. Moreover, the interconnect should be able to reduce the ohmic resistance across the interconnect to  $< 15 \text{ m}\Omega\text{cm}^2$  at  $750^\circ\text{C}$  and  $< 20 \text{ m}\Omega\text{cm}^2$  at  $850^\circ\text{C}$ . This work is directly linked to the project objectives 1b, 2a, and 2b. Overall, the WP progresses as outlined in the work plan. A summary of the status of relevant milestones (M) and deliverables (D) for the reporting period can be found in Table 5 and Table 6.

**Table 5. Deliverables in WP2, lead partner, and delivery dates.**

Del No	Title	Lead	Original date	Delivery date/ New date
D2.1	Deliver sheets of K44M steel for coating at SMT	APE	M3	M3
D2.2	Deliver SoA CeCo coated 441 steel (CS0)	SMT	M3	M3
D2.3	Deliver production scale CeCo coated K44M (CS1) to CU and DTU for testing, and to BOR for hydroforming	SMT	M6	M8
D2.4	New coating variations on 441/K44M (CS2) delivered for testing to CU and DTU	SMT	M9	M11
D2.5	Report on selection of substrate material and pre-treatment. Delivery of a corresponding steel coil to SMT for coating	APE	M12	M15
D2.6	Report on chemical stability of the coated interconnects (T2.3)	CU	M18	M19
D2.7	Report on mechanical properties of the coated interconnects (T2.4)	DTU	M18	M24



D2.8	Final iteration of steel and coatings (CS3) delivered for corrosion testing at CU, and mechanical and ASR testing at DTU	SMT	M26	M32
------	--	-----	-----	-----

**Table 6. Milestones in WP2, lead partner, and dates reached.**

MS No	Title	Lead	Original date	Date reached/ New date
M2.1	Coating-alloy combination (CS3) with ASR < 25 mΩcm <sup>2</sup> at 750 C and < 30 mΩcm <sup>2</sup> at 850°C manufactured and delivered for stack testing	SMT	M18	M24
M2.2	Final coating and steel generation (CS4) shown to reduce ASR < 15 mΩcm <sup>2</sup> at 750°C and < 20 mΩcm <sup>2</sup> at 850°C	CU	M36	M42
M2.3	Final coating and steel generation (CS4) with interface fracture energy above 8 J/m <sup>2</sup>	DTU	M36	M42

The main results to highlight are:

- A successful demonstration of the feasibility of using SoA high-volume roll-to-roll manufacturing methods for interconnect.
- A successful long-term test of the coated interconnect chemical stability for up to 3,000 hours, where the coatings decrease the chromium evaporation by at least 10 times. Investigations on old samples of Sanergy HT 441 proved the stability of the coating for 38,000 h.
- Once coated with a protective coating the low-cost steels AISI 441 and K44M perform equally good as the specialized steel Crofer 22 APU with respect to corrosion rate measured in the lab.

### T2.1 Requirement analysis and supply of steels

At the start of the project initial data indicated that uncoated K44M corrosion rate was only half that of Crofer 22 APU at 750°C. Based on these findings, the following material was delivered by APE (D2.1 and D2.5):

- 5 sheets of 1,000 by 1,250 mm sized K44M sheets, 0.5 mm thickness (Coil ref# 699453)
- 15 sheets (A4) K44M sheets in 0.3 mm thickness (Coil ref#71818AB)
- 1 coil (1 ton) of K44M, 400 mm width 0.5 mm thickness (Coil ref#938972)

The composition for the steels used in the project can be found in Table 7.



**Table 7 Composition of the used batches in the project**

	C	Si	Mn	Cr	Mo	Ti	N	S	P	Nb
#699453 0.5mm	0.013	0.37	0.35	18.82	1.858	0.003	0.015	0.0005	0.021	0.562
#71818AB 0.3mm	0.015	0.40	0.35	19.03	1.86	0.0055	0.020	0.0003	0.028	0.6
#938972 0.5mm	0.015	0.40	0.30	18.96	1.865	0.011	0.019	0.0017	0.024	0.586

Two low cost steels are used in the project K44M and AISI 441. Both of these materials are considered suitable for interconnect applications due to a high Cr and low Al content. Although both materials contain Si, the concomitant addition of Nb is expected to impede the formation of a detrimental layer of silica at the metal oxide interface. However, it was found (D2.6) that silica formation nevertheless occurred, which might result in increased ASR values.

## T2.2 Coating of interconnects

The major challenges of using ferritic stainless steels as SOC interconnect material are oxidation (leading to degradation and eventual failure), chromium evaporation (degrading SOC oxygen electrode), and oxide scale growth (increasing ASR). Highly protective coatings on interconnects are important to eliminate chromium evaporation, which reduces oxidation and oxide layer growth. SMT has developed a large-scale roll-to-roll process that allows for the production of PVD-coated material at a competitive cost. So far SMT has produced several coating variations on different substrates for the lab testing at the universities and hydroforming experiments. Coating of an entire steel coil in the production line is scheduled for early autumn 2020.

## T2.3 Corrosion testing

The performance of the substrate/coating combinations CS0 (Co/Ce coating on 441) and CS1 (Co/Ce coating on K44M) was validated in the laboratory at 750 °C and 850 °C, which are representative SOC stack temperatures of SOLIDpower and Sunfire stacks. Additionally, CS0 and CS1 were benchmarked against the Co/Ce coating on a Crofer 22 APU substrate, which is commonly used nowadays but prohibitive from a cost perspective. Oxidation kinetics and chromium evaporation studies were performed to understand the high temperature behavior of the substrate/coating combination for more than 3,000 hours. Details of the experimental methods used can be found in D2.6. The experimental results were correlated to the microstructure by chemical and morphological analysis in a scanning electron microscope (SEM) with energy-dispersive X-ray spectroscopy (EDX), leading to an understanding of the behaviour and chemical stability of the coated interconnects.

Figure 1 shows the net mass gain data of the uncoated and coated specimens exposed to 750 °C and 850 °C. Uncoated specimens (Figure 1a) of AISI 441 and K44M show significant differences in the net mass gains. At 750 °C, uncoated K44M showed a negative net mass loss after 500 hours, because of higher mass loss due to oxide vaporization than mass gain due to



oxidation. At 750 °C and 850 °C, AISI 441 exhibits higher net mass gains than K44M, indicating faster oxidation kinetics. However, the coated samples (Figure 1b) did not show such a difference in the mass gains, indicating similar oxidation kinetics. The coated commercial steels, AISI 441 and K44M, showed similar mass gains as the coated specialized steel, Crofer 22 APU, for up to 3,000 hours at both the exposed temperatures. Moreover, the chromia scale is thinner (=growing slower) on the coated specimens compared to the uncoated specimens. This indicates that the coatings are effective in reducing the oxidation kinetics of steel substrates and with a protective coating there is no significant difference in performance between the low-cost steels and the specialized steel Crofer 22 APU.

Figure 2 shows the chromium evaporation of the uncoated and coated specimens exposed at 750 °C and 850 °C. Uncoated steels K44M AISI 441 showed similar cumulative chromium evaporation at 850 °C after 500 hours (Figure 2a). However, at 750 °C, the chromium evaporation of uncoated K44M is higher than AISI 441. It is in fact approximately the same as both materials have at 850 °C. This peculiar behavior is currently under investigation. The high Cr evaporation of K44 M at 750 °C might be the reason for the low corrosion rate measured as mass gains that were observed before the start of the project, which led to the temporary conclusion that K44M has a lower oxidation rate than Crofer 22 APU. In the case of coated specimens (Figure 2b), chromium evaporation is reduced by at least a factor of ten for all investigated cases and a similar pattern evolves. At 850°C coated AISI 441 and K44M are almost identical in terms of Cr evaporation, while coated K44M exhibits slightly higher chromium evaporation than AISI 441 at 750°C. This might be related to the uncoated edges of the samples. The samples exposed for 3,000 hours were subsequently used of Cr evaporation measurements and the evaporation rate was similar to the one observed in the first 1,000 hours (Figure 2).

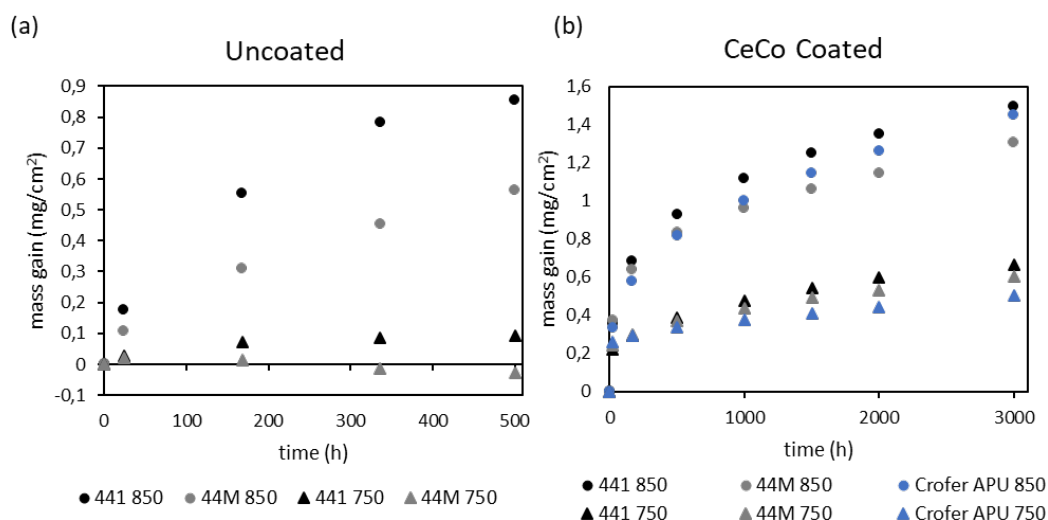
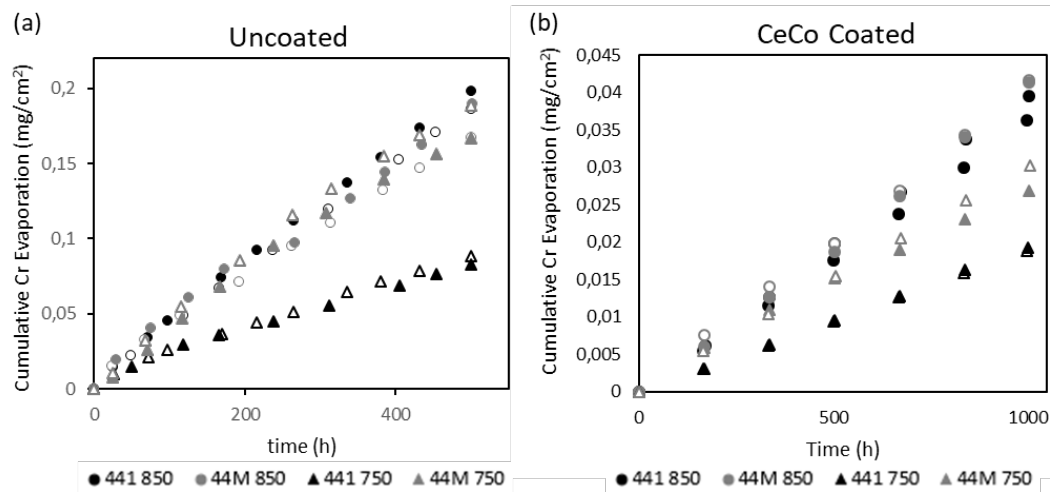
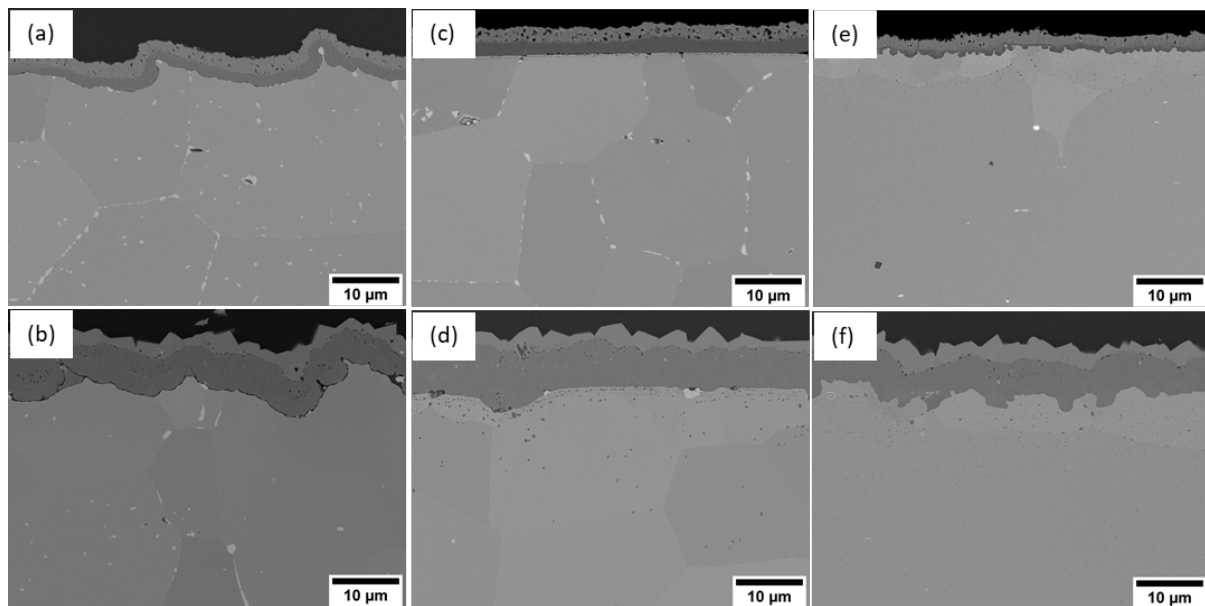


Figure 1. Net mass gain values of (a) uncoated and (b) coated steels exposed to 750°C (triangles) and 850 °C (circles) for up to 3000 hours in air with 3 % H<sub>2</sub>O.



**Figure 2. Cumulative chromium evaporation values of (a) uncoated and (b) coated steels exposed to 750 °C (triangles) and 850 °C (circles) for up to 1000 hours in air with 3 % H<sub>2</sub>O. Filled and empty symbols represent two individual isothermal exposures.**

Figure 3 shows SEM micrographs of the coated specimens exposed at 750 °C and 850 °C for 3,000 hours in the air with 3 % H<sub>2</sub>O. The micrographs revealed that the coatings are intact after 3,000 hours, and a continuous chromia layer is seen under the coatings. The coatings appear to be more porous at 750 °C and denser at 850 °C. The low cost steels, K44M and AISI 441 showed Laves phase precipitates in the steel matrix, which are coarser at 850 °C. Laves phase formation is typical for ferritic steels with Nb additions and increases the creep strength at higher temperatures. Due to a lack of Nb, the Laves phase precipitates are absent in Crofer 22 APU. The thickness of the oxide scales on coated AISI 441, K44M, and Crofer APU after 3,000 hours is 3-5 μm at 750 °C and 9-11 μm at 850 °C, which matches well with the observed mass gains.



**Figure 3. Ion milled cross sections of coated steels exposed in air with 3 % H<sub>2</sub>O for 3000 hours. (a) K44M at 750 °C and (b) K44M at 850 °C; (c) AISI 441 at 750 °C and (d) AISI 441 at 850 °C; (e) Crofer APU at 750 °C and (f) Crofer APU at 850 °C**

While the mass gains are similar for the coated steels, the structure of the oxide layer is slightly different between the AISI 441, K44M, and the specialized steel Crofer 22 APU. Due to the silicon (Si) content present in the steel (For composition refer to D2.6), a thin, slow-growing silica oxide layer forms at the metal/oxide interface in AISI 441 and K44M. However, such a layer is absent in Crofer 22 APU due to the very low Si content in the steel. The silica layer has a very high resistance; thus, it is detrimental to the cell resistance as it grows. Furthermore, the low CTE of silica can easily cause oxide scale spallation. Nb is known to form Laves phase precipitates that bind Si and thus reduce the rate of silica layer formation. Although Nb is present in the steels, AISI 441 and K44M, it is not enough to inhibit entirely the formation of the silica layer.

To circumvent this problem Nb containing coatings have been investigated (Figure 4a) to explore whether a Nb containing coating has the ability to inhibit the silica layer formation at the metal/oxide interface by a Nb containing coating. Figure 4b shows the cross-section EDX maps of the Co-Ce-Nb coated AISI 441 exposed for 1,000 hours at 850 °C. Initial results show that Nb is accumulated at the metal/oxide interface, where usually the silica layer is found. This indicates that it might be possible to impede the formation of silica by the addition of Nb via a coating layer. However, further investigation is in progress to understand the interaction of Si and Nb and their influence on the ASR of the coated steel. This coating is a candidate for further use in the project as well as a CeCo coating with a thicker Ce layer (50 nm instead of 10 nm). The 10 nm Ce layer was optimized for specialized steel and it thus conceivable that a higher Ce content will be beneficial for a rare earth element (RE) free steel like AISI 441 or K44M. Currently both coatings are under investigation and a down selection process will be carried out on which coating option to proceed with.

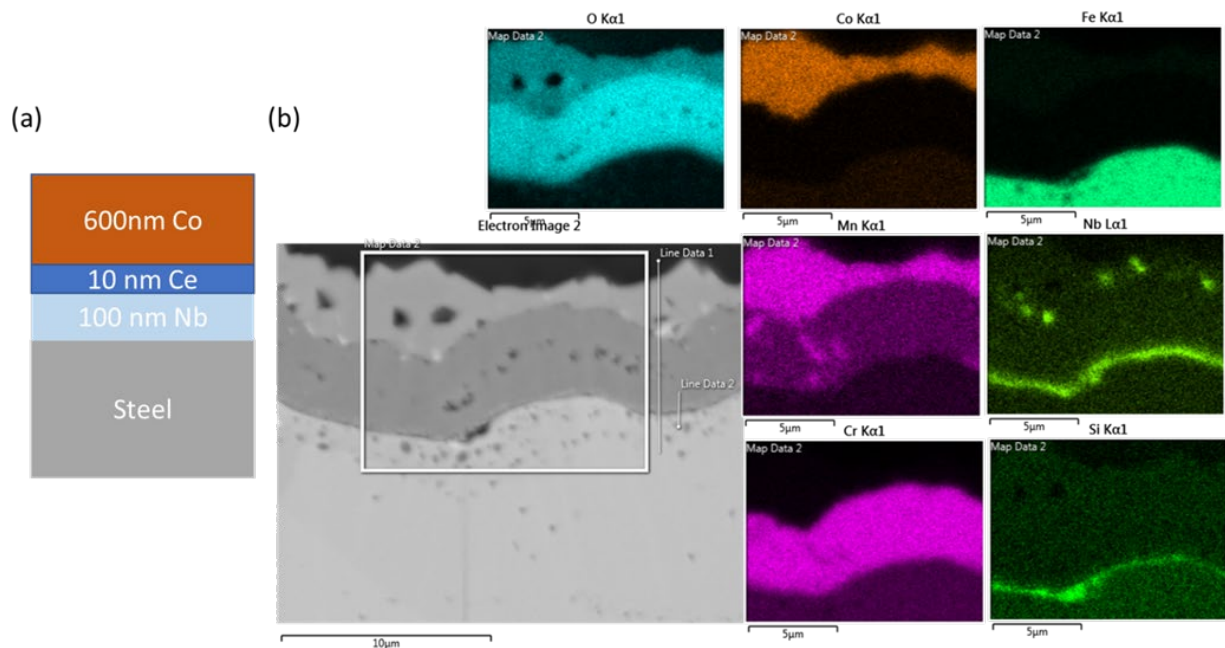


**Figure 4. (a) Coating structure with 600 nm Co, 10 nm Ce and 100 nm Nb on AISI 441 (b) Cross-section EDX maps of Co-Ce-Nb coated AISI 441 exposed to 850 °C for 1,000 hours in atmosphere with airflow containing 3 % H<sub>2</sub>O.**

#### T2.4 Mechanical Testing (DTU, APE)

In this task the mechanical adherence at 750 °C and 850 °C of the CoCe-coating on the AISI 411 steel from Sandvik, marketed as Sandvik Sanergy® HT 441 has been evaluated. For this, a glass-ceramic sealant with high fracture energy (i.e. 23.7 J/m<sup>2</sup> [1]) is joined to coated steel bars in a sandwiched structure. When broken apart, the intent is to have the coating pulled off the steel substrate because of the strong adherence to the glass. The robust glass-ceramic sealant applied in this work thus acts as a “glue” between the top and bottom steel bars. The robustness of the coated layer and crack propagation path are investigated using four-point bending, and fractography analyses are used to investigate if the fracture occurs in the coating/steel interface. Details can be found in D2.7.

The experimental procedure was thus: I. Screen printing ink and substrates, II. Sample preparation (screen printing and sintering), III. Four-point bending test and IV. SEM and EDX analysis of the fractured surfaces.

Figure 5 shows the room temperature fracture energy of the sandwiched samples after 250 h of aging at 750°C and 850°C. The inherent fracture energy of the V11 glass, as reported in [1] is also presented in the figure. As seen, the fracture energy of the sandwiched samples increased with the aging temperature.

<sup>1</sup> I. Ritucci, K. Agersted, P. Zielke, A.C. Wulff, P. Khajavi, F. Smeacetto, A.G. Sabato, R. Kiebach, A Ba-free sealing glass with a high coefficient of thermal expansion and excellent interface stability optimized for SOFC/SOEC stack applications, Int. J. Appl. Ceram. Technol. 15 (2018) 1011–1022.

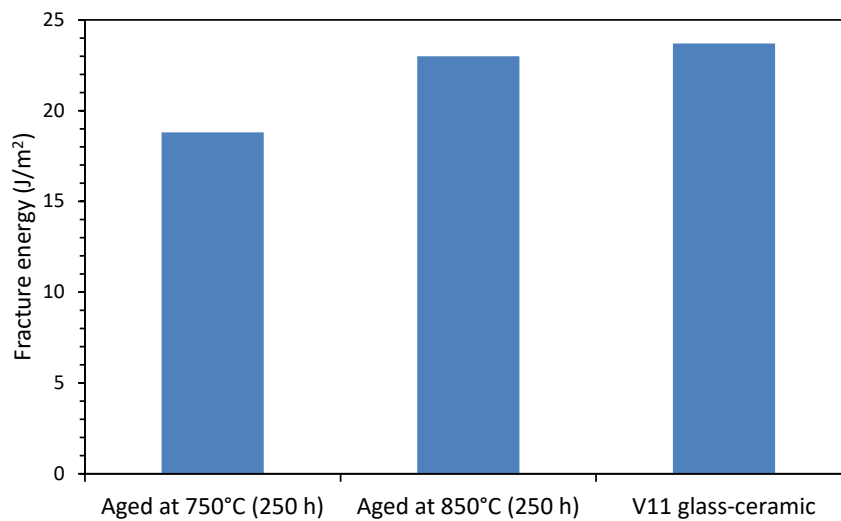


**Figure 5. Fracture energy measured at room temperature for glass-ceramic sandwiched coated steel 411 samples after aging at 750°C and 850°C for 250 h in air, and the inherent fracture energy of the used glass-ceramic reported in [1].**

SEM micrograph and EDX analysis of the top fractured surface are presented in Figure 6. Elemental analysis shows the presence of Si near the two edges of the fractured surface, while Mn and Cr are found between the Si rich areas. Hence, it is clear that the crack has propagated partly through the glass layer and partly through the oxide layer/substrate interface of the CoCe-coated 441 substrate.

From Figure 5 it is seen that the fracture energy of the sandwiched samples is comparable to the inherent fracture energy of the V11 sealant. Accordingly and since the crack has propagated through the oxide and glass layers (as found by the elemental analysis), the fracture energy of the CoCe-coated 441 steel interconnects interface is concluded to be comparable to that of the V11 glass, i.e. 20-23 J/m<sup>2</sup>.

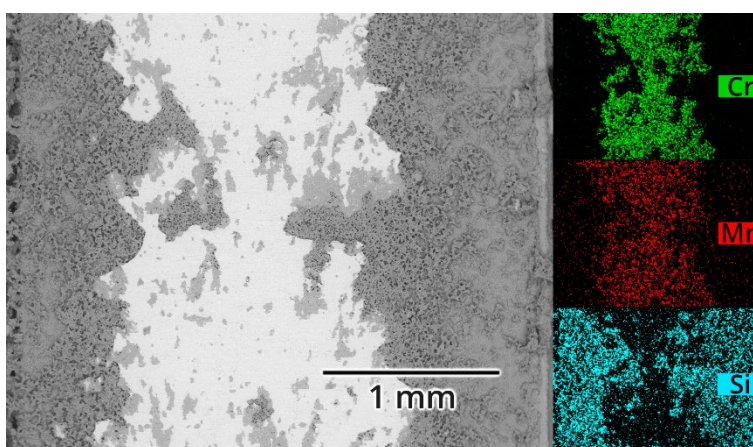


**Figure 6. SEM micrograph and elemental analysis of the fractured surface of the top (long) bar after the four-point bending test.**



The measured fracture energy is thus well above the values reported for preoxidized Crofer 22 APU (15.9 J/m<sup>2</sup>) and MnCo<sub>2</sub>O<sub>4</sub>-coated Crofer 22 APU (13.6 J/m<sup>2</sup>); and comparable to that of alumina-coated Crofer 22 APU (23.7 J/m<sup>2</sup>) [4]. The adherence of the coating of on the steel of the cost-effective Sandvik Sanergy® HT 441 interconnects solution is hence concluded comparable to other state-of-the-art interconnect / coating solutions.

### 1.2.3 WP3 - interconnect design and shaping

#### Executive summary of WP3

The objective of the activities in this WP is in the first step to develop a new design of the interconnect with an optimized flow distribution resulting in reduced max. stresses by 30 %. The development will be based on the very efficient 3D multiphysics model developed at DTU that considers couplings between flow, heat transfer, mechanical stresses and electrochemical reactions. The corresponding flow simulations will ensure that the pressure drop will be maintained low. In the second step, the interconnects will be produced and delivered to the stack manufacturer (SUN). An overview of the status of relevant deliverables and milestones for this reporting period is shown in Table 8 and Table 9.

**Table 8.** Deliverables in WP3, lead partner, and delivery dates.

Del No	Title	Lead	Original data	Delivery date/ New date
D3.1	Flow distribution for the current SUN stacks computed by the multiphysics homogenized SOC stack model and delivered to FZJ for comparison with detailed model	DTU	M9	M15
D3.2	The optimized interconnect geometry delivered to FZJ for detailed computational studies and further refinement geometry	DTU	M18	M22
D3.3	CAD drawing of the optimized SUN interconnect geometry delivered to BOR for hydroforming	FZJ	M21	M27
D3.4	Hydroformed pre-coated test interconnects with various shaping depths, slopes and curvature radii delivered for investigation at CU and BOR FZJ	BOR	M9	M12
D3.5	Report on the corrosion properties of the hydroformed pre-coated interconnects tested after shaping	CU	M12	M17



**Table 9.** Milestones in WP3, lead partner, and dates reached.

MS No	Title	Lead	Original data	Date reached/ New date
M3.1	Optimized interconnect flow field achieved, with stress in the cell-interconnect interfaces reduced by 30 % compared to that from current interconnect design, while maintaining a pressure drop below 30 mbar	DTU	M18	M24
M3.2	Optimized interconnect manufactured and sent to SUN for implementation in stacks	BOR	M24	M30

Due to the COVID-19 pandemic there has been some adaptation to the approach of the activities in T3.1/T3.2/T3.3. Since the DTU 3D Multiphysics model was not ready early this year and to avoid further delay, full 3D flow simulations have been started at FZJ. Different options for the channel design have been simulated to analyze their effect on the pressure drop. Different options for optimizing the channel geometry analyzed together with BOR. In the meantime BOR carried out forming tests on samples in order to check the limits and to get design limitations from a manufacturing point of view. The requirement by the stack producer to use 0.5 mm thick steel sheet for the interconnect made it more challenging to shape the desired geometries. However, a novel solution to mitigate this challenge has been proposed, which has now been agreed upon amongst the involved partners. The feasibility of producing the novel design solutions will be investigated in the near future. An interconnect with dummy channels will be designed in order to manufacture some samples and to prove the manufacturability.

Now, the 3D Multiphysics model have been completed and will used to determine the flow distribution and result to the final optimized interconnect geometry (D3.2). The new interconnect will be made by the new material chosen in WP2.

Overall, and despite the difficulties caused by the Corona crisis, the activities have made a very good progress. The 3D Multiphysics model (D3.1) has been completed and optimization of geometry can now be performed. The flow distribution model is set-up and aligned with the real stack conditions. Samples are manufactured for further analysis (WP2) and first design rules are defined. The investigation of the samples of the pre-coated steel sheets showed a similar chromium evaporation to the undeformed coated steel sheets. Therefore the shaping of the interconnects do not affect the chrome evaporation protection.

### **T3.1 Optimization of the interconnect to minimize thermal gradients in SOFC operation**

For this task a multi-physics model of the Sunfire stack, which is used as an example, is needed. This model must be fast enough to simulate the influence of various geometric changes for an entire commercial stack (30 cells). Thus, the newly developed homogenization approach<sup>2</sup> was used to model the various interacting physics of the SOFC stack, i.e. flows,

---

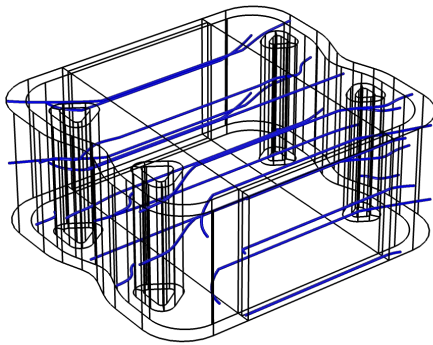
<sup>2</sup> M. Navasa, X.-Y. Miao, H.L. Frandsen, A fully-homogenized multiphysics model for a reversible solid oxide cell stack, Int. J. Hydrogen Energy. 44 (2019) 23330–23347.



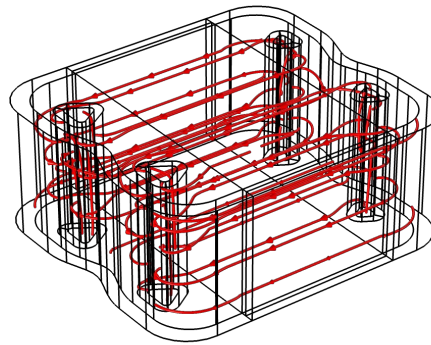
electro-chemical reactions, heat current and mass transport, as well as mechanical stresses. The purpose of this task is to minimize the mechanical stresses by modifying the interconnect geometry to minimize the temperature gradients.

The flow field of the Sunfire stack was simulated and delivered in D3.1 by DTU for comparison with a more detailed single repeating unit at FZJ in T3.2. To simulate the flow in the manifolds various attempts for circumventing simulating the complex turbulent flow with the computationally demanding Reynolds-averaged Navier-Stokes equations (RANS) have been made. One of these attempts, which was not successful, could be used for simulating heat exchangers, and a paper on this has been submitted and is currently in review. A reasonably fast method for simulating the turbulent free flow in the manifolds was eventually found, which will be used onwards in the project. Consequently, other the simulation of other physical phenomena have been added to be able to simulate the multiphysical response of the Sunfire stack, see Figure 7.

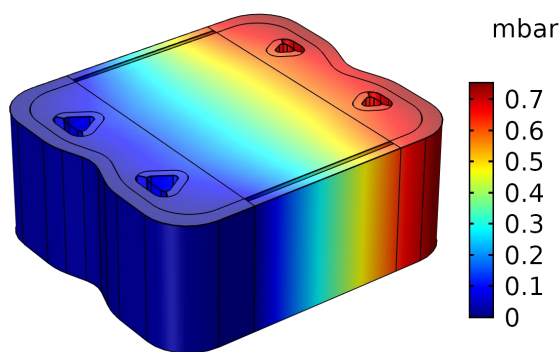
a) Flow field on the air side



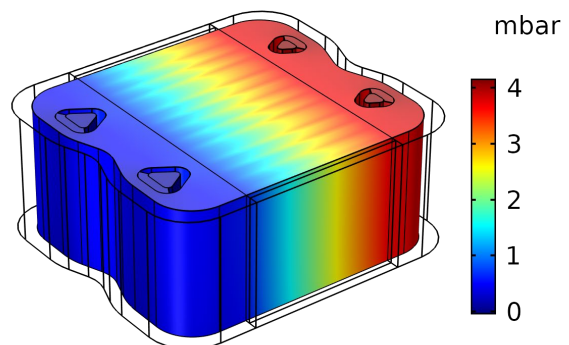
b) Flow field on the fuel side



c) Pressure variation on the air side [mbar]



d) Pressure variation on the fuel side [mbar]



e) Hydrogen molar fraction

f) Current density variation [A/cm<sup>2</sup>]

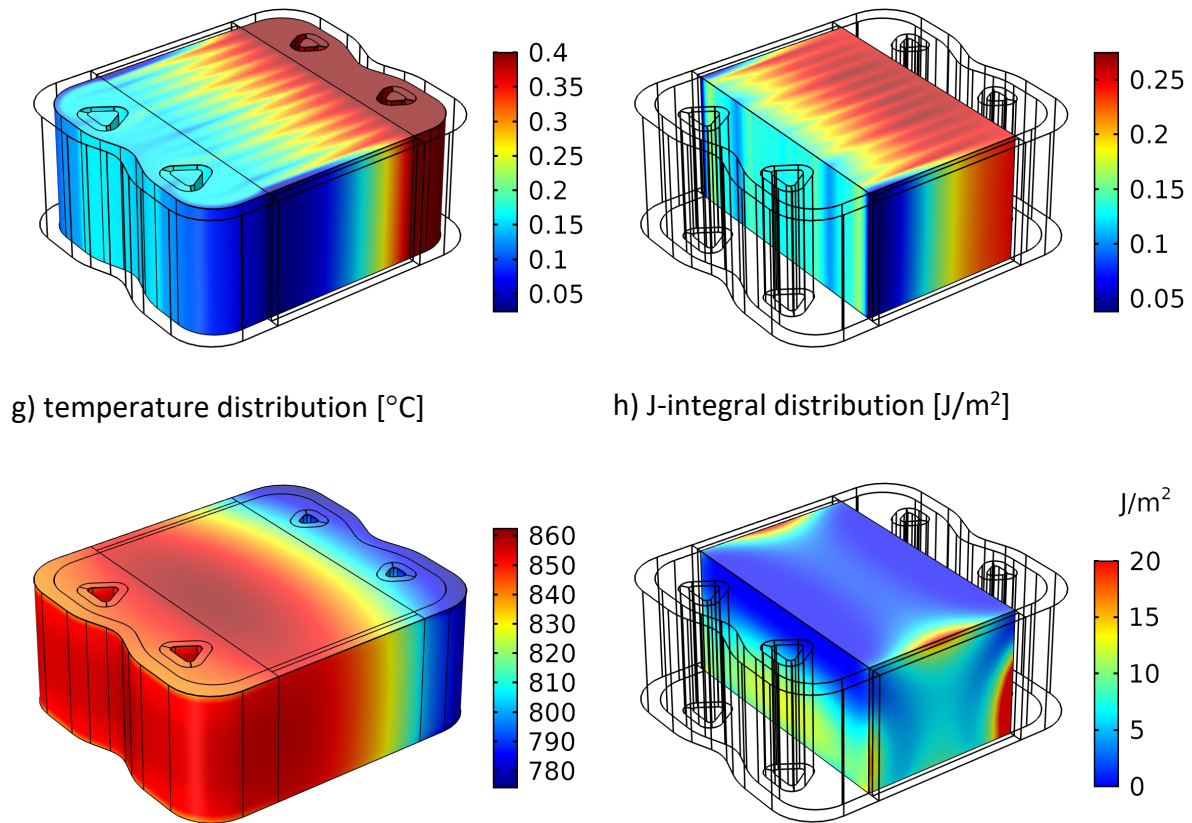
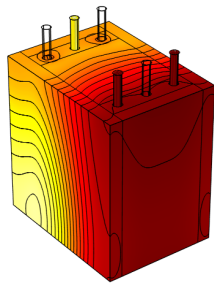


**Figure 7 Output from the Comsol Multiphysics stack model a) Stream lines of the air flow field, b) stream lines of the fuel flow field, c) pressure variation on the air side, d) pressure variation on the fuel side, e) hydrogen molar fraction, f) current density variation, g) temperature distribution, h) J-integral distribution.**

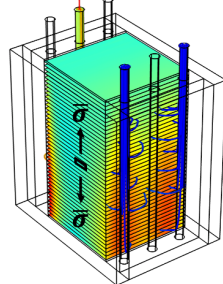
To simulate the local fracture in the homogenized stack model, where all stresses are evenly distributed, a method was developed within the project to simulate the local stresses from the average stresses, using so-called localization. This entails imposing the average stresses on the boundary of a sub-model representing the local repeating geometry with the critical zone to be investigated further. A novel method of mapping the average stresses to the local stresses at the critical zone was developed and furthermore this was also used to map the average stresses to the so-called J-integral or energy release rate, see Figure 8. Both the maximum local stress (strength) and the critical energy release can be used as criteria for determining the fracture at the cell-interconnect interface, but the latter is a more robust measure as strength varies significantly for ceramic components. The critical energy release rate (fracture energy) for the contact layer / interconnect interface is also the quantity measured in WP4 for the novel contact layers, tying experimental and modelling work together. A paper on this novel localization method is currently in preparation.



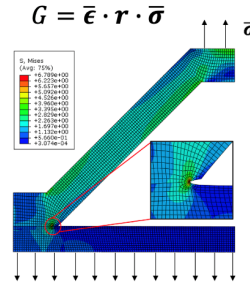
a) Multiphysics, incl. temp,  $T$



b) Average stress distribution,  $\bar{\sigma}$



c) Localisation via mechanical sub-model  
 $G = \bar{\epsilon} \cdot r \cdot \bar{\sigma}$



d) Local energy release rate,  $G$ , in stack

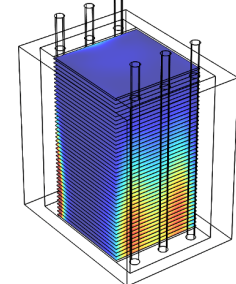


**Figure 8. Localization approach for retrieving local stresses and J-integral from average stresses  $\bar{\sigma}$ .**

The next steps in this task are to use the developed homogenized multiphysics model of the SUN stack and establish a method for investigating different channel geometries (D3.2). From the various geometries the one yielding the lowest thermo-mechanical stresses will be provided to FZJ for further design optimization together with BOR in T3.2.

### T3.2 Detailed shaping and modelling of interconnect design optimized for SOFC operation

The aim of task 3.2 is to compute and investigate the flow distribution and pressure drop in the repeating unit of the SUN stack. This is done in FZJ with a Navier-Stokes approach using a conventional computational fluid dynamics model. Later on, the channel and interconnect geometry will be optimized taking into account the allowable radii of curvature and pressing depth. The permeabilities that are used in the flow simulations will be applied in the 3D multiphysics model at DTU in order to find a distribution of permeabilities that gives the least stresses. This will result in a proposal for the distribution of permeabilities which can be used at FZJ for simulations to propose indentations to a final interconnect design to be produced with BOR. A full 3D-CAD model will be the output.

The numerical grid for the simulation was created using ANSYS Mesh. For grid independence studies, four different mesh configurations were used. Since the design of the stack is symmetrical, only half the stack layer is modelled. The boundary condition "symmetry" is assigned to the cut surface. The numerical model for the simulation was created in ANSYS FLUENT V19.2.

#### Pressure distribution of air side

The simulations of pressure drop were carried out with different meshes with the same boundary conditions, see Table 10. The pressure distribution for Mesh 1 is shown in Figure 9.

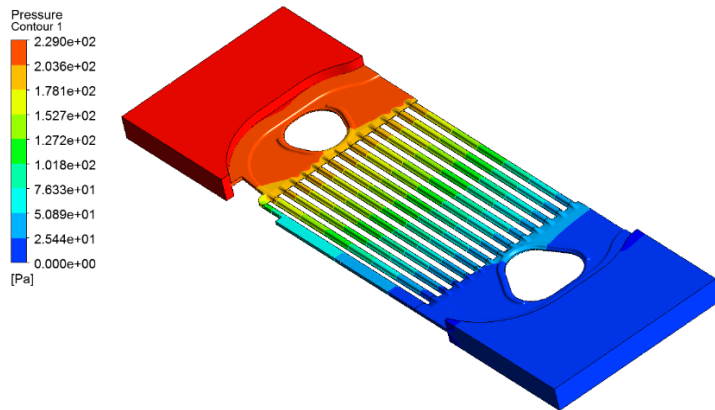


**Figure 9. Pressure distribution along the air side of the stack (with Mesh 1)**

The pressure loss in the entire air layer for different grid configurations is shown in Table 10.

**Table 10. Pressure loss of the layer for all mesh configurations.**

Result	Mesh 1	Mesh 2	Mesh 3	Mesh4
Pressure loss of layer (Pa)	229	229	219	234

These simulations reveal that the results are largely independent of the mesh configuration.

**Flow distribution between the channels on air side**

The next step is to consider the flow distribution between the individual air channels. The distribution calculations were carried out for all mesh configurations and are shown in Figure 10.

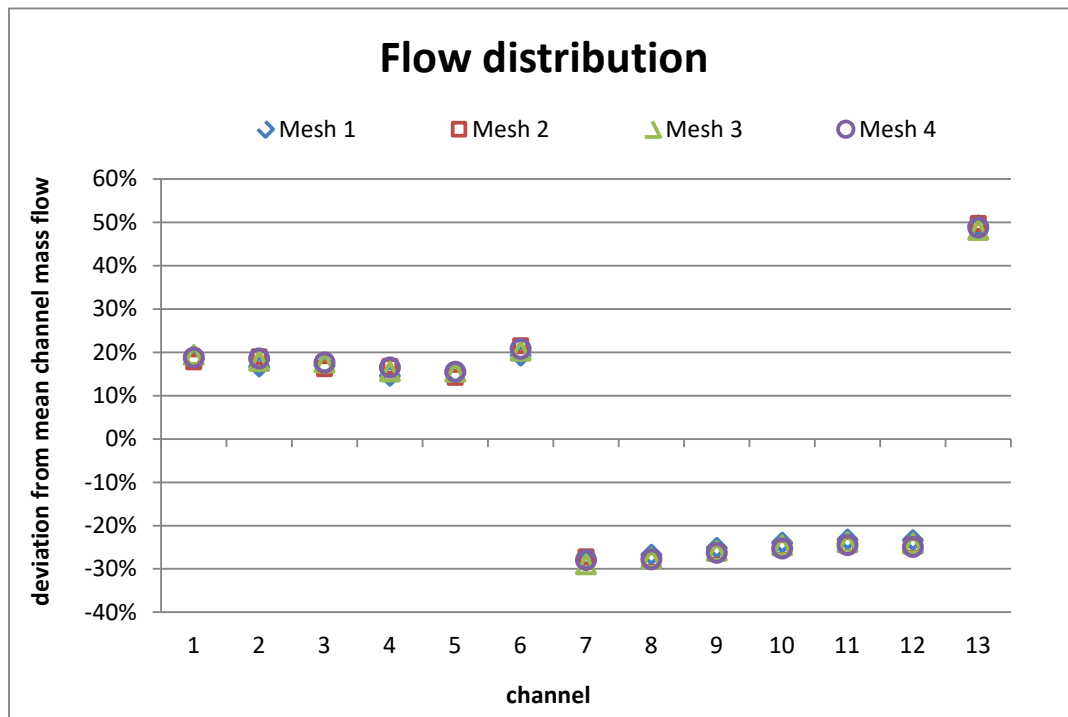


**Figure 10. Flow distribution over the air channels for different mesh configurations**



The flow distribution mainly corresponds to the cross-sectional area of the channels, the small difference in mass-flow among the channels. These calculations again confirm that the results are independent from the mesh configuration. It is sufficient to carry out future calculations with computational grid created with three elements across a gap and three inflation layers.

### Pressure distribution of fuel side

The pressure distribution is shown in Figure 11.

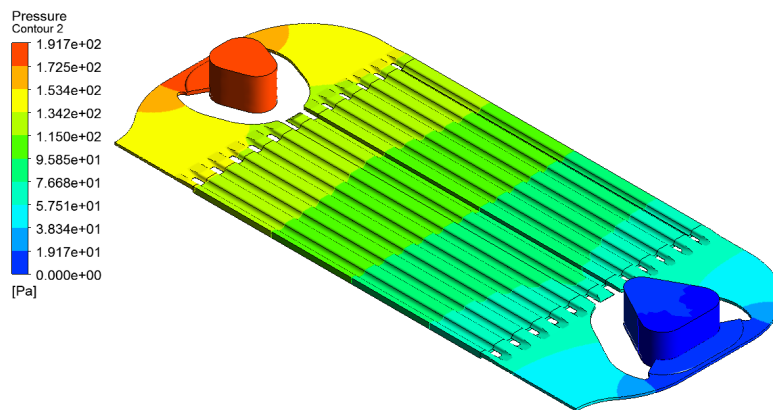


Figure 11. Pressure distribution along the fuel side of the stack

The pressure loss in entire fuel layer is 190.7 Pa.

### Flow distribution over the porous segments on fuel side

The velocity distribution in Figure 12 shows that in the porous segments lying opposite the valley of the channel have higher velocities and therefore also higher mass flow rates than those lying opposite a mountain. For this reason, the gas flow is strongly directed towards the valley segments. However, according to experience of Sunfire, this effect does not lead to significant performance drop of the stack.

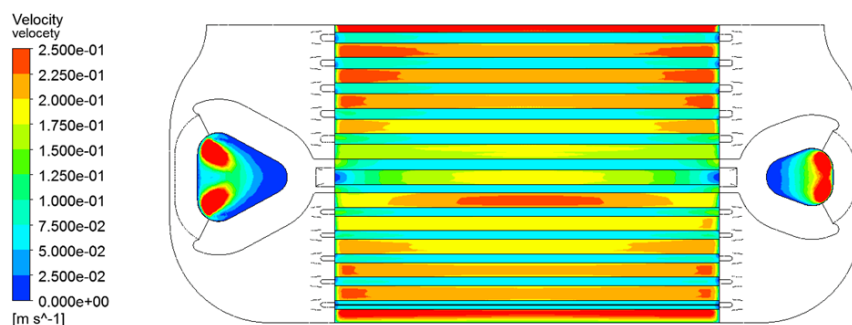
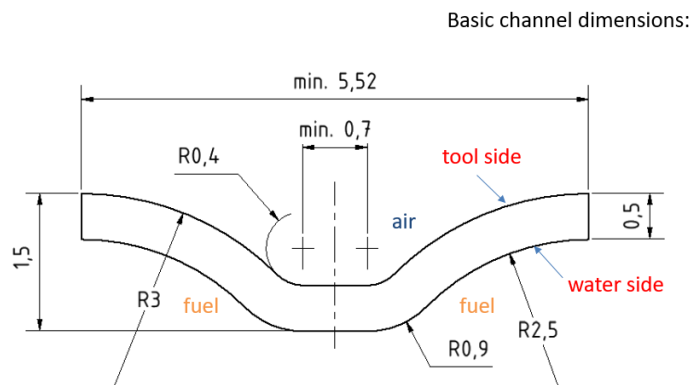


Figure 12. Velocity distribution over all porous segments of the fuel side



### Channel design options

In order to optimize the airflow distribution in the repeating unit it is planned to adjust the channel geometries accordingly. Because of the difficulties in deforming the 0.5 mm sheet the degree of deformation is almost limited to the dimensions shown in Figure 13.



**Figure 13. Basic channel geometry**

The aim for the channel layout is to keep the unsupported distance for the cell as small as possible. For this reason, it still must be checked whether the minimum distance from 0.7 mm can be further reduced towards zero. If it is possible from a manufacturing point of view, the unsupported distance would decrease from 5.52 mm to 4.82 mm. In the following sections, possible design variations are explained step by step.

#### Channel design option 1

In principle the horizontal sections of the channel can be extended by  $\Delta y$  and  $\Delta x$ , see Figure 14. The change by  $\Delta y$  leads to wider the fuel gas channel, which is not critical. The increase  $\Delta x$  increases the unsupported distance and is therefore not preferable.

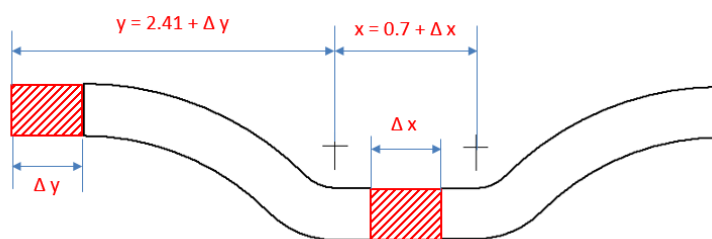


**Figure 14. Channel design option 1**

#### Channel design option 2

In principle the geometry can be manipulated by changing the large radius of the channel, see Figure 15.

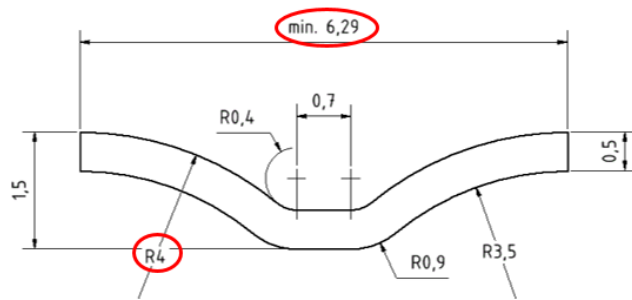


**Figure 15. Channel design option 2**

Figure 15 shows the effect while increasing the radius from 3 mm to 4 mm. If this method is used, the unsupported distance increases from 5.52 mm to 6.29 mm at the same time, which also does not lead to the desired result.

### Channel design option 3

With option 3, all air channels have the same cross-section, with a feasible minimum of unsupported distance. The different pressure losses are generated by indentations of variable depth ( $\Delta y$ ) and/or length ( $\Delta x$ ), see Figure 16.

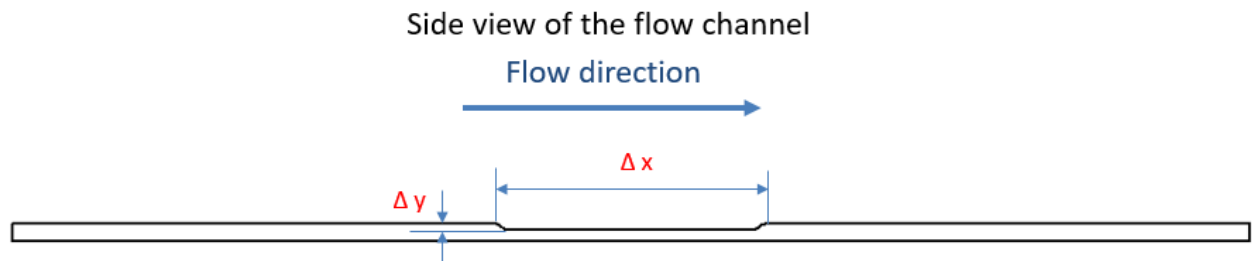


**Figure 16. Channel design option 3**

A first impression of how this method can work is given in Figure 17. It shows pressure drop results for two different indentation depths and lengths up to 45 mm. This method will give sufficient options for adjusting the pressure loss in combination with the minimum unsupported distance of the cell.



### fluid volume of air channel

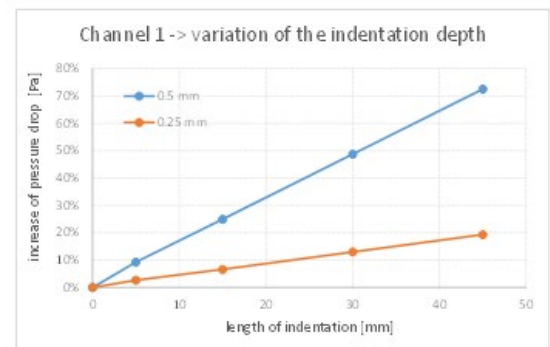
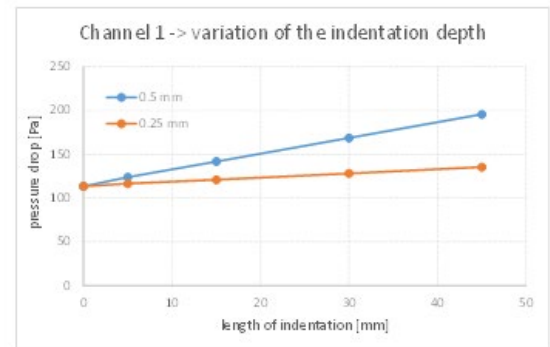
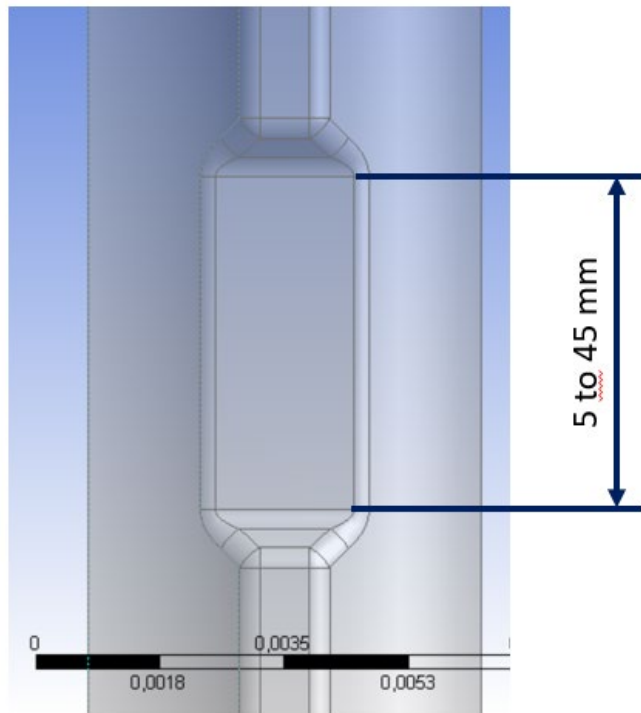


Figure 17. Channel design option 3

### Conclusion and outlook

The flow distribution and pressure loss of the current repeating unit of the Sunfire stack were investigated. These results will be used to validate the homogeneous stack model of DTU and as a reference for the design of the future channel geometry.

The options for designing the channel geometry are currently being discussed between the partners. Once the decision for one of the options has been made, the detailed simulations are carried out.

### T3.3 Shaping of interconnects by hydroforming

At the beginning of the project, BOR in collaboration with FZJ, SAN and DTU has designed a test shape of the pre-coated steel to investigate the shaping limits of the steels and coatings. This is done to support the design of new interconnects in T3.2. For comparison and due to the fact that the SUN stack design applies 0.5 mm thick metal sheets, the tests have been performed with 0.3 mm SoA coated 441, 0.5 mm coated 441 and 0.3mm uncoated Crofer 22H. The tests aim to investigate the parameter window for manufacturing (pressing depths, slopes, curvature radii).

Borit has designed and milled a test tool based on the Sunfire interconnect design. Figure 18 shows the design and the area selected for the forming trials as this includes all relevant features of the entire design.

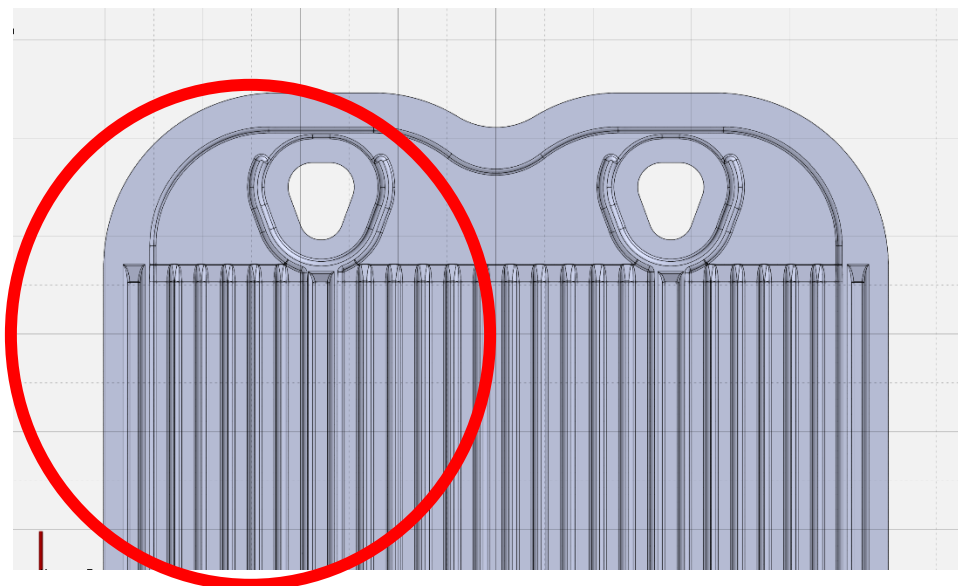


**Figure 18. Design of the interconnect and area selected for the forming tests**

Using this tool, samples of coated 441 in 0.3 and 0.5 mm thickness and Crofer22H 0.3 mm were produced. For all materials, the forming did not show any problems with respect to cracking the material as evident from Figure 19 and Figure 20 shown below. Measurements were then performed to investigate and quantify the achieved shape and to guide the design of the new interconnect, taking the production constraints into account. From these measurements it can be concluded that the achieved depth is almost independent of the material, indicating that the Hydrogate process can be used without any issue to form the Sunfire interconnect in the two tested materials. As expected, the achieved radii at the bottom of the channels are depending on the material thickness.

The formed samples were sent to Chalmers and FZJ for further investigation of the influence of the forming process on the material and coating.



**Figure 19. Formed samples in coated 441, 0.3 mm**



**Figure 20. Formed samples in coated 441, 0.5 mm**

### **T3.4 Evaluation of hydroformed interconnects and coatings**

The aim of task 3.4 is to evaluate the influence of shaping process on the material and coatings in relevant operating conditions simulated in the laboratory. The performance is determined by benchmarking the Cr vaporization rates to that of non-deformed samples. Details of the experimental methods used can be found in D3.5.

Precoating and subsequent shaping have the advantages of reducing the costs and streamlining the production. However, shaping of the coated steel results in cracks and delamination of the coating (Figure 21a), especially in the areas subject to severe deformation. This, in turn, leads to higher chromium evaporation and oxidation rates, a concern for the long-term operation of stacks.

Nevertheless, chromium evaporation experiments (Figure 21b) showed a higher rate of chromium evaporation during the initial 50 hours, which quickly decreased to levels similar as measured on undeformed CeCo coated steel.

Furthermore, the cross-section micrographs (Figure 21c) and EDX analysis (Figure 21d) showed a continuous cobalt layer on the entire surface. The smaller cracks are healed by the volume expansion of the metallic coating upon oxidation, whereas the interdiffusion of the spinels  $(\text{Co,Mn})_3\text{O}_4$ ,  $(\text{Cr,Mn})_3\text{O}_4$  on the surface healed the larger cracks. Interdiffusion led to the formation of a uniform  $(\text{Co,Cr,Mn})_3\text{O}_4$ , reducing the chromium evaporation, protecting the bare steel only after 50 hours into the exposure.

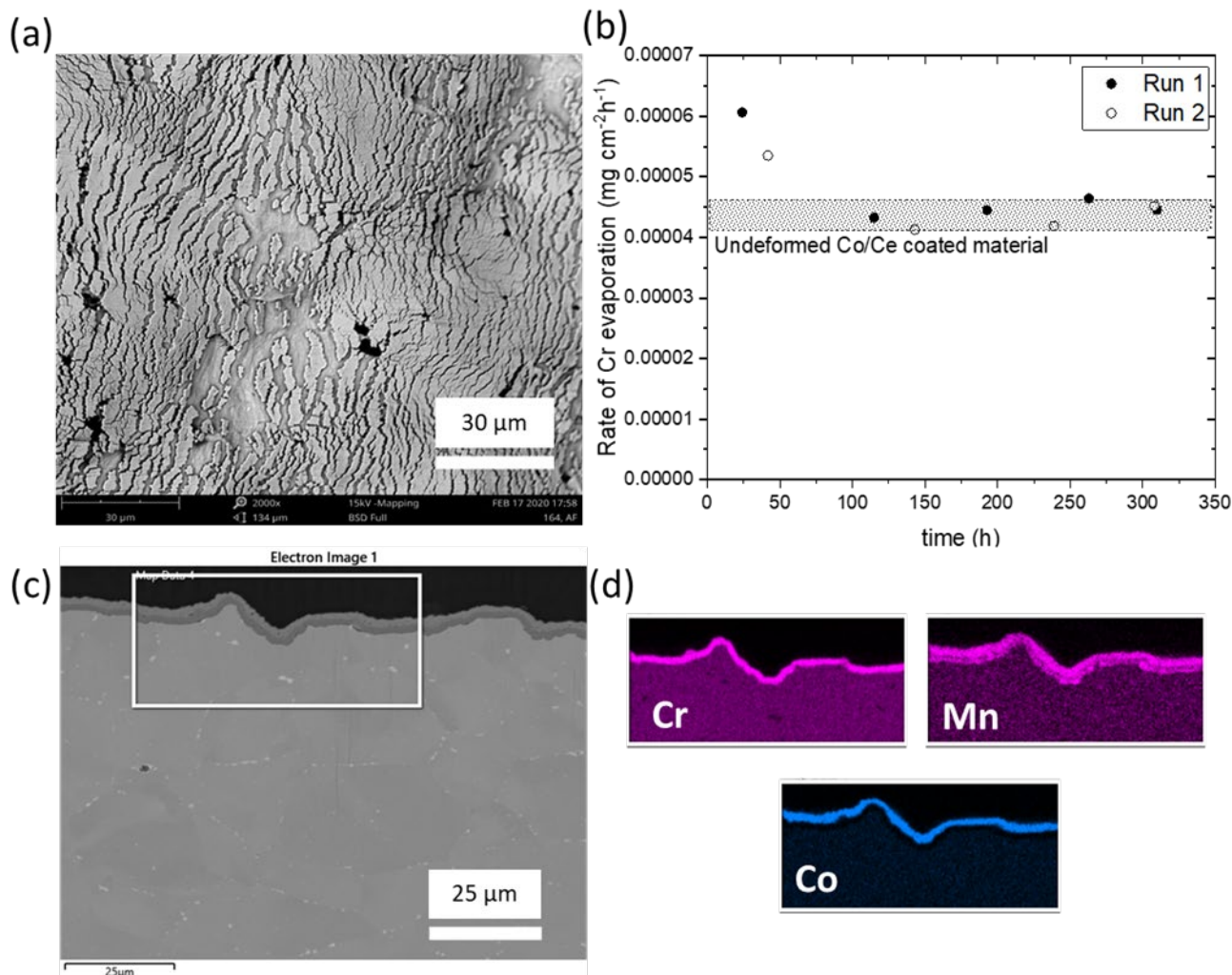


**Figure 21 (a) SEM micrograph showing the surface morphology of the coating after shaping operation (b) Rate of chromium evaporation (c) SEM micrograph of ion milled cross-section (d) EDX maps of Cr, Mn and Co of the shaped interconnect exposed for 310 hours in air with 3% H<sub>2</sub>O**

#### 1.2.4 WP4 - Development of robust contact layers

##### Executive summary of WP4

The overall objective of WP4 is to develop a novel, robust contact solution for the contact between the interconnect and the oxygen electrode. The optimized contact layer (CL) should have an improved mechanical stability (>200 % over SoA) and chemical compatibility with the interconnect. Another goal is to make this available for cheap mass manufacture through high-throughput ink-jet printing. The work is related to the project objectives 1a, 1b, 1d and 2b. Overall, the WP progress are as outlined in the work plan. An overview table with the status of relevant deliverables (D) and milestones (MS) for this reporting period can be found in Table 11 and Table 12.



**Table 11 Deliverables in WP4, lead partner, and delivery dates.**

Del No	Title	Lead	Original date	Delivery date/ New date
D4.1	Report on ASR with the different chemical compositions and particle sizes measured at initial operation and after 3000 hours of aging	DTU	M12	M12
D4.2	Report on fracture energy of the cell interconnect interface with the different chemical compositions and particle sizes measured at initial operation and after 3000 hours of aging	DTU	M12	M24
D4.3	Deliver optimized contact layer (CL2) in sufficient amounts to SUN and SOL for screen printing and incorporation into their full stacks	DTU	M24	M24
D4.4	Report on the feasibility and accuracy of the high-speed DoD inkjet printing of known ceramic inks onto SOC interconnects	TI	M9	M9

**Table 12 Milestones in WP4, lead partner, and dates reached.**

MS No	Title	Lead	Original date	Date reached/ New date
M4.1	First version of the contact layer paste (CL1) delivered to SUN and SOL for screen printing in their short stacks	DTU	M9	M12
M4.2	Second version of the contact layer paste (CL2) delivered to SUN and SOL for screen printing in their full stacks	DTU	M18	M24
M4.3	Proof-of-concept for the use of high-speed DoD inkjet printing achieved	TI	M18	M24
M4.4	High-speed DoD inkjet printing used to print contact layers on 50 interconnects for full stacks and send to SOLIDpower and Sunfire	TI	M27	M33
M4.5	ASR of stack element using the best contact paste (CL3) measured over 3000 h and degradation rate shown to be less than $<5 \text{ m}\Omega\text{cm}^2$ per 10 thermal cycles at $750^\circ\text{C}$ and $850^\circ\text{C}$	DTU	M33	M39
M4.6	Fracture energy of the cell interconnect interface using the best contact paste (CL3) measured and shown to be $> 200 \%$ higher than SoA contact layers ( $3 \text{ J/m}^2$ ) after 3,000 hours of aging at $750^\circ\text{C}$ and $850^\circ\text{C}$	DTU	M33	M39

All relevant deliverables (D4.1, D4.2 and D4.4) have been handed in. D4.2 is considered partly fulfilled due to challenges with sample preparation and the consequent emergence of the



Corona pandemic. MS 4.1 were reached, while MS 4.2 and onwards is delayed due to the Corona pandemic. Explanations on delays and contingency strategies can be found in the corresponding work tasks (WTs) below. The main results to highlight are:

- A successful long-term test of the cathode contact layer for 3,000 h with very low degradation rates ( $-0.1 \text{ m}\Omega\text{cm}^2/1000 \text{ h}$ ) and low area specific resistance ( $12 \text{ m}\Omega\text{cm}^2$  @  $850 \text{ }^\circ\text{C}$ , target  $25 \text{ m}\Omega\text{cm}^2$ )
- An increase in fracture toughness of the relevant interface up to 800 % (target 200 %)
- A successful proof-of-concept printing campaign through high-throughput ink-jet printing

#### T4.1 Contact layer formulation and application in stacks (DTU, TI, SUN, SOL)

Novel contact layer solutions based on the concept of *reactive oxidative bonding* are the core of this WT. In this method, the contact layer is applied in the form of metal particles, which during SOC stack assembly and operation ( $750\text{-}850 \text{ }^\circ\text{C}$ ) are oxidized in-situ to form dense and well-conducting oxides, as outlined in Figure 22.

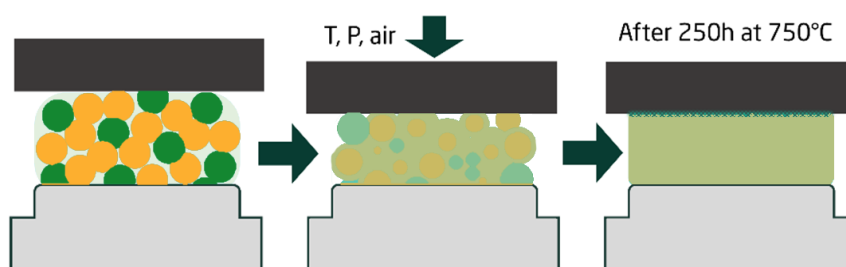


**Figure 22. Schematic illustration of the reactive oxidative bonding concept for fabrication of tougher contact layers**

The *first version* of contact layers (CL1) is based on metallic precursors (Mn, Co and Cu), mixed in the stoichiometric ratios to form  $\text{MnCo}_2\text{O}_4$  and  $\text{Cu}_{1.3}\text{Mn}_{1.7}\text{O}_4$ . The compositions were chosen as both oxides have an appreciable electrical conductivity and thermal expansion coefficient. Due to the high reactivity of the metallic precursors, a strong bond is created to both the coated interconnect and the SOFC electrode. Promising results in terms of electrochemical performance (see WT4.2 below) and fracture toughness (see WT4.3 below) were achieved.

After initial validation at DTU, the first version of the contact layer paste (CL1) was shipped (with a delay of 2.5 month) to Sunfire and SOLIDpower (MS 4.1) for further testing in stacks in WP5. Initial work on the second generation of contact layers (CL2) started at DTU, but a 6 month delay is expected for MS 4.2 and future milestones due to the Corona pandemic.

To shorten the delay, experiments on the second version CL2 will be carried out/started, without having final results from stack testing of CL1. By changing from the serial workflow outlined in the original work plan to this parallel approach, it is expected to minimize the delay to 6 months. The increase in risk by this strategy is considered moderate, as any relevant findings from the stack test can be considered in the final version of the contract layer (CL3).



## T4.2 Interface chemical stability (DTU, CU)

In order to validate the performance of CL1, the area specific resistance (ASR) was measured over an assembly consisting of the coated interconnect (AISI 441, Sandvik Materials), the contact layer material and an oxygen electrode. Details on the experimental methods used can be found in D4.1. The chemical stability of the contact layer/interconnect interface was evaluated by post-test analysis by SEM and EDS.

The ASRs of the different interfaces during isothermal aging at 750 °C in air are shown in Figure 23. The average ASR values recorded at start and the end of the measurement, and the degradation rate calculated from the slope of the curve during the last 500 h of the measurement are summarized in Table 13.

It should be noticed that during the initial 1,000-2,000 h of aging, the ASR decreased due to improvement of the area of contact and improved conductance of the green and only mildly sintered interconnecting LSM layers (mimicking an oxygen electrode). This effect is well-known and related to the experimental setup. The ASR of the uncoated 441 steel corresponds to the grey line, while data for AISI 441 with CeCo coating (Sandvik materials), but no contact layer, are depicted in cyan. Samples of uncoated AISI 441 steel with the Mn-Cu or Mn-Co contact layer are represented by the dark yellow and the green line, respectively. Results for AISI 441 with CeCo coating and cathode contact layers are shown as yellow line for Mn-Cu and light green-grey line for Mn-Co.

The ASR of the uncoated AISI 441 (grey line, Figure 23) increased rapidly from the start. Comparing the ASRs measured for samples *with* (green, light green brown and yellow) and *without* the contact layer (blue), it is clear that the contact layer does not contribute significantly to the cross-plane resistance.

Applying the Mn-Co (green line) or Mn-Cu (dark yellow line) contact layers directly to the AISI 441 steel results in low and more stable ASRs. The best performance in terms of ASR is achieved by combining the contact layer with a CeCo coating (Sandvik Materials) on the AISI 441 steel. The CeCo coating is needed for reducing the release of poisonous Cr(VI)-species from the interconnect (see WP2).

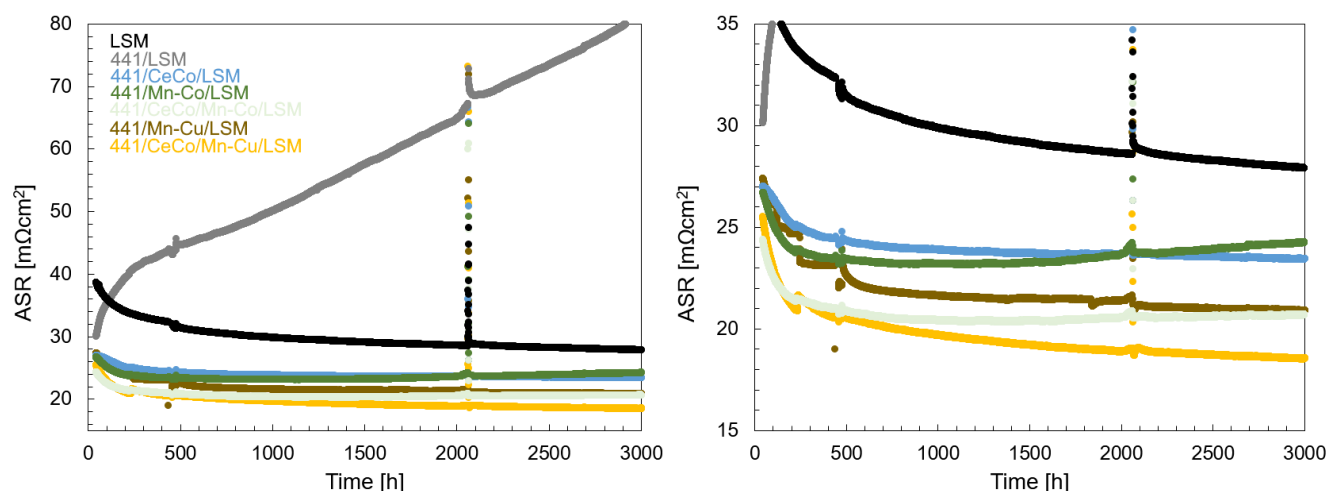


**Figure 23.** ASR measured in air at 750 °C. Right side plot shows an excerpt of the ASR between 15 and 35  $m\Omega cm^2$



A similar ASR measurement was carried out at 850 °C, the key findings are summarized in Table 13. After ca. 2,500 h of testing, the measurements became slightly unstable and were therefore terminated after a total of 2,750 h at 850 °C. As for the measurement at 750 °C, the lowest ASR and degradation rate was measured for the interfaces with a Mn-Cu contact layer.

**Table 13 Area specific resistance (ASR) after assembly and 3,000 h and corresponding degradation rate.**

ASR @ 750 °C Interface	Initial ASR [mΩcm <sup>2</sup> ]	ASR after 3,000 h [mΩcm <sup>2</sup> ]	Degr. rate [mΩcm <sup>2</sup> /1,000 h]
LSM	39	28	-0.7
441/LSM	31±3	70±16	8.8
441/CeCo/LSM	29±3	25±3	-0.3
441/Mn-Co/LSM	27±1	25±1	0.8
441/Mn-Cu/LSM	27±1	21±1	0.3
441/CeCo/Mn-Co/LSM	25±1	19±2	0
<b>441/CeCo/Mn-Cu/LSM</b>	<b>24±2</b>	<b>18±1</b>	<b>-0.3</b>
ASR @ 850 °C Interface	Initial ASR [mΩcm <sup>2</sup> ]	ASR after 2,750 h [mΩcm <sup>2</sup> ]	Degr. rate [mΩcm <sup>2</sup> /1,000 h]
LSM	8.4	4.4	0.3
441/LSM	31±1	N/A	> 1000
441/CeCo/LSM	14±1	25±28	16±22
441/CeCo/Mn-Co/LSM	11±2	16±1	1.2±0.5
<b>441/CeCo/Mn-Cu/LSM</b>	<b>14±4</b>	<b>12±1</b>	<b>-0.1±0.5</b>

The Mn-Cu contact layer has a high affinity for Cr and thus increased the diffusion of Cr from the chromia scale into the contact layer, also when the steel was coated with CeCo. This leads to a higher Cr activity in the near surface layer that is potentially of concern for long-term operation of stacks with the Mn-Cu contact layer due to increased Cr poisoning. In order to evaluate this, a CeCo coated AISI 441 sheet was coated with Mn-Cu contact paste and exposed for 1,000 h at 850°C and subsequently tested in a Cr evaporation test rig at CU.

It was found that the evaporation rate is about a third of the uncoated material or almost 4 times higher compared to the CeCo material without CuMn paste (Figure 24). In order to reduce this effect, the Ce layer thickness was increased from 10 nm to 50 and 200 nm, respectively, because Ce proved an efficient diffusion barrier in earlier studies. However, this did not result in the desired reduction of Cr diffusion into the CuMn layer.



In another experiment the CeCo coated material was preoxidized before application of the CuMn paste, as it was hypothesized that the initial metal/metal contact is most detrimental for the interdiffusion. However, even with this precaution substantial amounts of Cr were detected in the outer CuMn-oxide layer. Currently this problem is not solved and a Cu free contact paste might be the better solution, or if fracture toughness is prioritized a somewhat higher Cr evaporation might have to be tolerated.

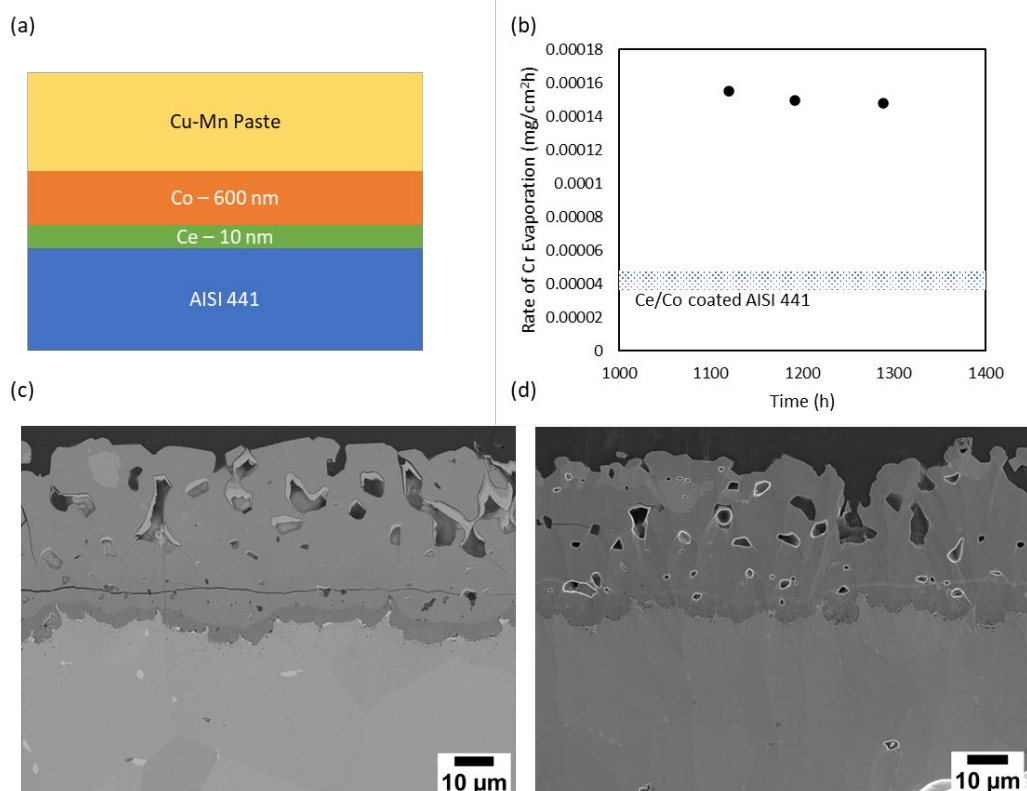


**Figure 24 (a) Coating structure with 600 nm Co, 10 nm on AISI 441 (CS0) with Cu-Mn paste (b) Chromium evaporation of a sample with of contact paste applied after 1000 hours of exposure at 850°C in air with 3 % H<sub>2</sub>O with a flow rate of 6,000 sml min<sup>-1</sup>. (c) Ion milled cross section of Mn-Cu contact paste applied on Sanergy 441 HT, exposed for 1,000 hours at 850°C. (d) Ion milled cross section of contact paste applied pre-oxidized Sanergy 441 HT exposed for 500 hours at 850°C**

Compared to the work plan, WT 4.2 is very well on track. In fact targets expressed in objective 1c (reducing the Ohmic resistance across the interconnect to < 20 mΩcm<sup>2</sup> at 850°C (evaluated after 3,000 h)) have been already reached. Initial experiments on thermal cycling relevant for MS 10 (M33) showed also promising results, leading to the expectation that no delays in the future will occur.

### T4.3 Mechanical testing of contact interfaces (DTU)

To evaluate the adhesion of the contact layers to the steel interconnect, the fracture energy was evaluated by four-point bending experiments (details on the method can be found in D4.2). The two different contact layers, Mn-Co and Mn-Cu, were applied on two different



ferritic stainless steels, 441 (Sandvik Materials) and K44M (Aperam), both without any coating and coated with CeCo (Sandvik Materials). Two trends could be observed among these eight samples:

- i) Using a CeCo coating on the steel increases the robustness, and
- ii) contact layers based on Mn-Cu have a higher fracture energy than Mn-Co based ones.

Consequently, the 441 ferritic steel with CoCe coating was selected as substrate for further aging tests. The results after 250 h of aging for Mn-Cu and Mn-Co are shown in Figure 25.

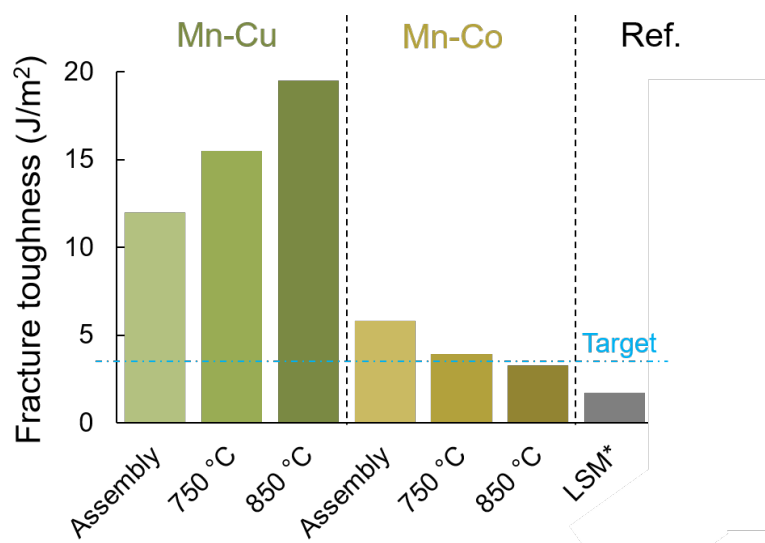


**Figure 25. Fracture toughness of Mn-Cu and Mn-Co contact layers on CoCe coated 441 ferritic steel after assembly and aging for 250 h at 750 °C and 850 °C. State-of-the-art LSM contact layers are added for comparison/as reference. The project target is displayed as dotted cyan line.**

The fracture energy of Cu-Mn contact layers increased by aging: the samples aged for 250 h at 750°C and 850°C had a fracture energy of 15.7 and 19.4 J/m<sup>2</sup>, respectively. This is approximately 35 % and 65 % higher than the fracture energy of the as-sintered samples. Interestingly, an opposite trend was found for Mn-Co. Here the fracture energy decreased after aging (Figure 25). Detailed results are reported in D4.2.

Compared to state-of-the-art, these results are very promising, and already now the < 200 % increase in mechanical fracture energy of the cell-interconnect contact (targeted in objective 1a and MS 11) has been achieved. Delays in relation to the work plan occurred as followed: The promised testing of samples aged for 3,000 h has not been carried out yet, until now only results after 250 h of ageing are available. The reason for the delay was the relocation of lab facilities at DTU and the COVID 19 lockdown. Experiments are ongoing now, and the results will be available 10/2020. This delay is expected to have little impact, as the development of the second generation of contact layers is already ongoing (see T4.1).



#### T4.4 Contact layer deposition by advanced manufacturing (TI, DTU)

The goal of this work task is to demonstrate that the contact layer formulation can be applied by advanced manufacturing techniques used in mass production. In the reporting period, proof-of concept experiments with existing ceramic inks from TI using high throughput ink-jet printing were successfully carried out on interconnects from SOLIDpower. No apparent issues in applying the inks occurred, the desired layer thickness (between 30 and 60  $\mu\text{m}$ ) was achieved (Figure 26) in two passages in the printer.

Details are reported in D4.4 and MS8 is considered fulfilled in time. Modifying the ink for the metallic particles used in the contact solution has already started, future deliverables and milestones are expected to be reached as planned and described in the work plan.

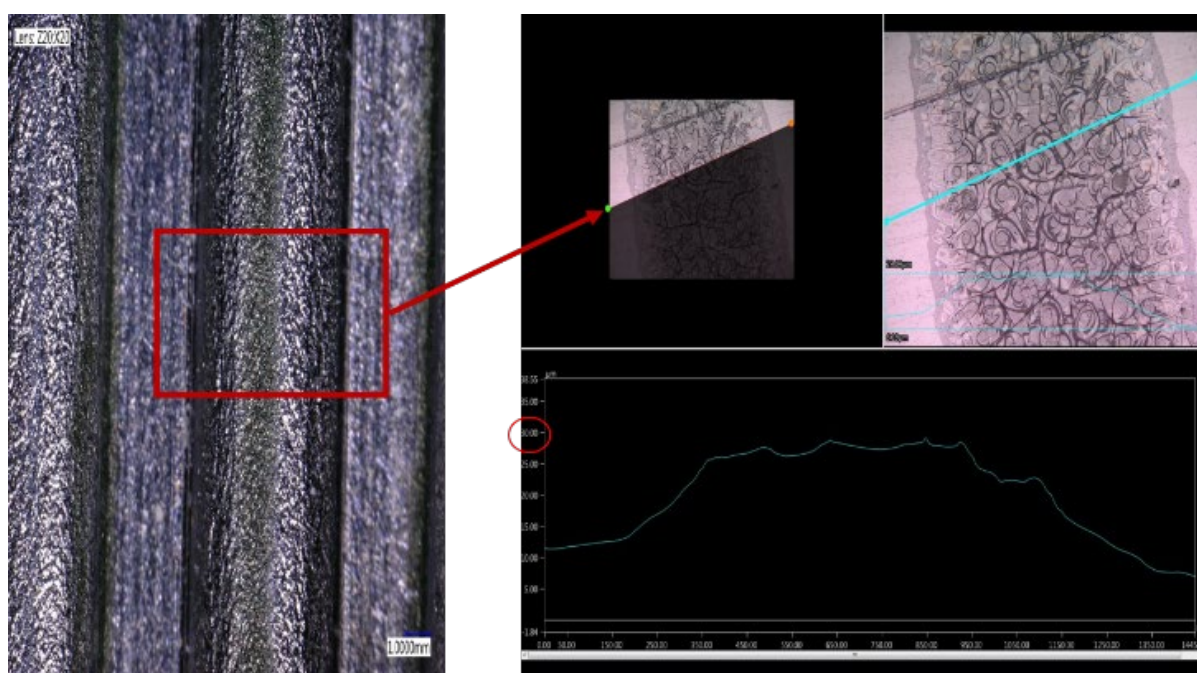


Figure 26. Left: Ceramic ink deposited on contact point (long rib) of a SOLIDpower interconnect, image with higher magnification and area used for profilometry (cyan line) top right. The height ( $> 30 \mu\text{m}$ ) of the print can be observed from the cross-section in the bottom right.

#### 1.2.5 WP5 - Production and testing of SOC stacks

##### Executive summary of WP5

The state-of-the-art (SoA) stacks (ST1) were successfully built using Sanergy<sup>®</sup> 441 HT as interconnect steel/coating solution. Where this could be done on schedule at SUN, challenges occurred at SOL resulting in some delay, see Table 14. It was found that the standard shaping method at SOL resulted in a high scrap rate using the Sanergy<sup>®</sup> HT 441 product from SAN. The SOL stack is now completed and currently being tested at FZJ.



The first stack from SUN (ST1) was tested for 3,500 h. The Sanergy® HT 441 with CeCo-coating showed a 50 % higher degradation of ASR compared to Crofer with MCF coating. Parts of the SUN stack were delivered to DTU and FZJ (D5.2) for postmortem analysis.

The second set of stacks (ST2) with new contact layers from SUN and SOL (D5.3) are delayed and will be delivered nine months later. This is primarily due to the Corona pandemic but also due to some concerns regarding the chemical expansion of the new contact layer. These are currently being investigated. The testing will therefore also be delayed by nine months (D5.4). This can however be fitted into the new proposed timeline of the project (see Section 5).

The rest of the WP is expected to be delivered on time with the extension asked for due to the Corona pandemic.

**Table 14. Deliverables in WP5, lead partner, and delivery dates.**

Del No	Title	Lead	Original date	Delivery date/ New date
D5.1	Deliver one (per stack manufacturer) short stack (ST1) with interconnects of 441 steel coated with CeCo at Sandvik for testing	SOL	M6	M11, M16
D5.2	Deliver tested sectioned stack with SoA coatings and test reports to FZJ and DTU	SUN	M12	M15, M21
D5.3	Deliver one (per stack manufacturer) short stack (ST2) with new contact layer CL1 for testing	SOL	M12	M21
D5.4	Deliver tested sectioned short stacks with CL1 and reports on thermal cycling testing results to DTU	SUN	M18	M27
D5.5	Deliver full stack (ST3) with different segments of SoA and new materials (per stack manufacturer) for testing	SOL	M24	M30
D5.6	Deliver one full stack (ST4) with different segments of SoA (per stack manufacturer) for testing at the respective manufacturer.	SUN	M30	M36
D5.7	Report on testing and on post-mortem analysis of the two full stacks with different segments (ST3)	FZJ	M36	M42



**Table 15. Milestones in WP5, lead partner, and dates reached.**

MS No	Title	Lead	Original date	Date reached/ New date
M5.1	Post-mortem analysis and stack test results demonstrating the feasibility of the novel contact layers (CL1) and comparable corrosion resistance of Sandvik's CeCo coating (to SoA steels and coatings)	FZJ	M21	M30
M5.2	Improved cyclability of the new contact layers (CL2) demonstrated, achieving 20 % less Ohmic resistance over the >50 thermal cycles	SOL	M30	M36
M5.3	Improved cyclability of the new contact layers (CL3) and optimized interconnect demonstrated, achieving 30 % less Ohmic resistance over the >50 thermal cycles	SUN	M36	M42

### T5.1 Implementation in stacks

SUN and SOL received a coil of Sandvik Sanergy® HT 441 for the first stack (ST1).

At SUN it was decided to build a 30-layer stack (ST1) instead of a short stack for D5.1 to have the possibility to add some layers with the conventional Crofer 22 APU with MCF coating (SUN standard) as a reference in the stack. The stack was joined successfully, and all quality criteria were successfully met.

SOL produced 100 cassettes (interconnects) using an embossing process according to the standard SOLIDpower procedure. After manufacturing, the cassettes were subjected to a quality control (QC). Unfortunately, 95 % of the cassettes did not pass the QC because of gas leakage. These defects were probably originating from the mechanical deformation of the steel during the embossing process. The five cassettes found in spec were used to make the short stack ST1 to be tested at FZJ. In order to match the requirements of the qualification benches of both SOLIDpower and FZJ, a two clusters stack was assembled, consisting of five repeating elements made by Sandvik and 4 conventional repeating elements.

a) Sunfire stack



b) SOLIDpower stack





**Figure 27** First stacks (ST1) produced at a) SUN and b) SOL with Sandvik Sanergy® HT 441 for interconnects.

### T5.2 Stack testing

ST1 from SUN was tested in stationary mode for 3,500 h with the parameters defined in the Test-protocols ( $T_{\max}$  860°C, H<sub>2</sub>/N<sub>2</sub> 40/60; FU 75 %), see D1.1. No leakages occurred during the test. The linear degradation of the AISI 441 were 50 % higher than the Crofer 22 APU reference, see Figure 28.

The ST1 stack from SOL was sent to FZJ, who have built a separate test rig for SOLIDpower stacks for the testing in the current project. The stack is being tested with the testing parameters set in test protocol for the SOL stack ( $T_{\max}$  750°C, H<sub>2</sub>/N<sub>2</sub> 60/40; FU 80 %), see D1.1. The stack have currently been tested for > 1000 hours.

Therefore, the delivery of parts from ST2 to DTU (D5.4) will be delayed by nine months.

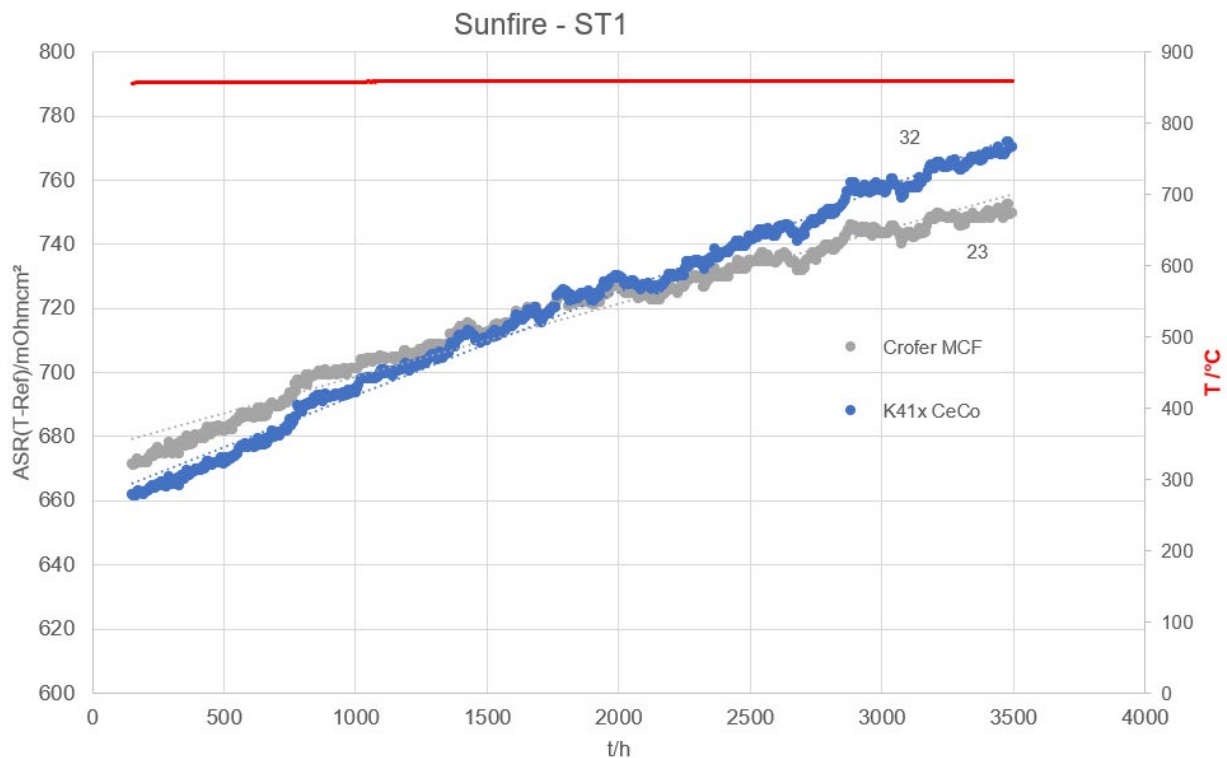


**Figure 28.** Degradation of SUN ST1 stack. The grey and blue lines show ASR increase over time for the two different steel/coating solutions, and the red line the temperature (K41x CeCo = Sanergy 441 HT).

### T5.3 Post mortem analysis

The stack was already disassembled at Sunfire. No cell breakages or leakages occurred. The cells of the Sanergy 441 HT layers showed dark stripes on the air-electrodes, which are assumed to be due to chromium evaporation. Samples for investigation of the substrate and coating were sent to DTU and FZJ, fulfilling D5.2.



## 1.2.6 WP6 - Techno-economic analysis

### Executive summary of WP6

The overall goal of WP6 is to put the technical improvements from the other WPs into monetary numbers to prove industrial relevance and applicability. Consequently, and simply put, the achievable profit and thus a successful business case for the manufacturer mainly depend on the product's prime cost (production cost + overheads). As most of the product's cost, prime cost as well as total cost of ownership, are already determined in early development phases, cost engineering parameters must be included in any preselection considerations to ensure cost-effective development of solutions. For this project, the first step was a high-volume production cost assessment for the SoA and the novel LOWCOST-IC route for 750 °C- and 850 °C ICs (D6.1). In course of this project, also a report on total cost benefits, an economy of scale study and the cost benefits due to increased lifetime will be assessed (D6.2). The work is related to the project objectives 2a, 2b and 2c. Overall, the WP progresses as outlined in the work plan. An overview table with the status of relevant deliverables (D) and milestones (MS) for this reporting period can be found in Table 16 and Table 17.

**Table 16 Deliverables in WP6, lead partner, and delivery dates.**

Del No	Title	Lead	Original date	Delivery date/ New date
D6.1	Report on break down of cost on the SoA and the LOWCOST-IC processing routes	AVL	M15	M21
D6.2	Report on total cost benefits taking into account processing routes, scale of economy and demonstrated technical improvements from LOWCOST-IC	AVL	M36	M42

**Table 17 Milestones in WP6, lead partner, and dates reached.**

MS No	Title	Lead	Original date	Date reached/ New date
M6.1	Show by break down of costs and economy of scale analysis that the cost will be reduced to < 5 € per unit of interconnect including coatings and contact materials for processing at 50 MW/year capacity	AVL	M18	M24

All relevant data is sent to the partners and preliminary estimates shows that MS 6.1 could be fulfilled, but further investigations are needed. D6.1 is delayed due to problems when setting up additional required bilateral NDAs and the Corona pandemic. The main results to highlight are:

- The breakdown of costs on SoA and LOWCOST-IC is calculated and distributed



- It is shown, that the IC production cost can be reduced to < 5 €/IC for a production volume of ICs for 50 MW/year electricity production.

## T6.1 Break down of cost

### Approach

The used software for this task, Siemens Teamcenter and Product Cost Management (TcPCM), is a cost simulation tool that uses a bottom-up process-oriented overhead calculation. For each part, AVL performed the following steps: First, the raw materials for the product were selected and afterwards, one or more manufacturing processes with machines, tools and human resources were set up. Machines, raw material data and general boundary conditions are provided by a database maintained by Siemens. Furthermore, the supplier structure was simulated by addressing in-house production costs by adding up materials plus manufacturing costs and sales prices by additionally adding overheads and profit. Overheads e.g. include sales, general and administration (SG&A), research and development (R&D) and interests. Figure 29 depicts the general bottom-up costing approach.



**Figure 29. Bottom-up costing approach of TcPCM**

This project can be categorized as fine estimation, because several pieces of information are not available or have to be generalized for the study not to be restricted to one product but show general importance for interconnect production instead. This includes:

- No exact interconnect design was used
- The overhead structure was not customized to the LOWCOST-IC supplier structure, but general overheads were used instead.
- The production processes in industry are not yet industrialized to very high volumes. A high-volume production facility and its cycle times had to be assumed to simulate the production of interconnects for 50 MW/year electricity production.
- The LOWCOST-IC process is yet to be demonstrated.

Such a fine estimation to generally compare manufacturing processes is a typical step in early product development. This is very important because, most of a product's prime costs are already determined in early development phases. Later, as product maturity rises, cost



engineering data becomes more precise, but the possibilities to reduce costs decrease as more boundary conditions are set.

For this study, the boundary conditions in Table 18 were used. They are common boundary conditions for high-volume production in Europe and do NOT represent the actual interconnect market right now. This was done to assess the scalability to high volumes of the SoA and the LOWCOST-IC production route.

**Table 18. Boundary conditions for cost calculation.**

General boundary conditions	Scenario I
Annual volume	ICs for 50 MW/year electricity production
Lifetime	8 years
Number of manufacturing lots	24 lots/year
Shift model	3 shifts/8 hours/5 days/48 weeks
Production hours	5,760 hours/year
Production site	Czech Republic
Efficiency factor Production & Assembly	80 %
Tooling	Calculated – one-time payment for first tooling set; further sets allocated

For overheads, the structure in Table 19 was used.

**Table 19. Overhead structure used for LOWCOST-IC.**

Overheads	Scenario I
Material overhead costs	4 %
Residual manufacturing overheads	25 %
Sales and general administration costs (SG&A)	10 %
Research and development (R&D) costs	5 %
Transportation costs	1,5 %
Profit	8 %

Next, raw materials and manufacturing processes as well as supply chain structures for the given products were set up. In this case, a 750 °C-and an 850 °C interconnect were chosen. Inputs for raw materials prices, manufacturing processes, tools, machine prices and cycle times were chosen in close contact with the according supplier representant of the LOWCOST-IC consortium. To match a 50 MW/year production volume, the processes and the supply



chain were adapted to fit a best-practice European high-volume approach. A visualization of all inputs needed for the cost calculation is shown in Figure 30.

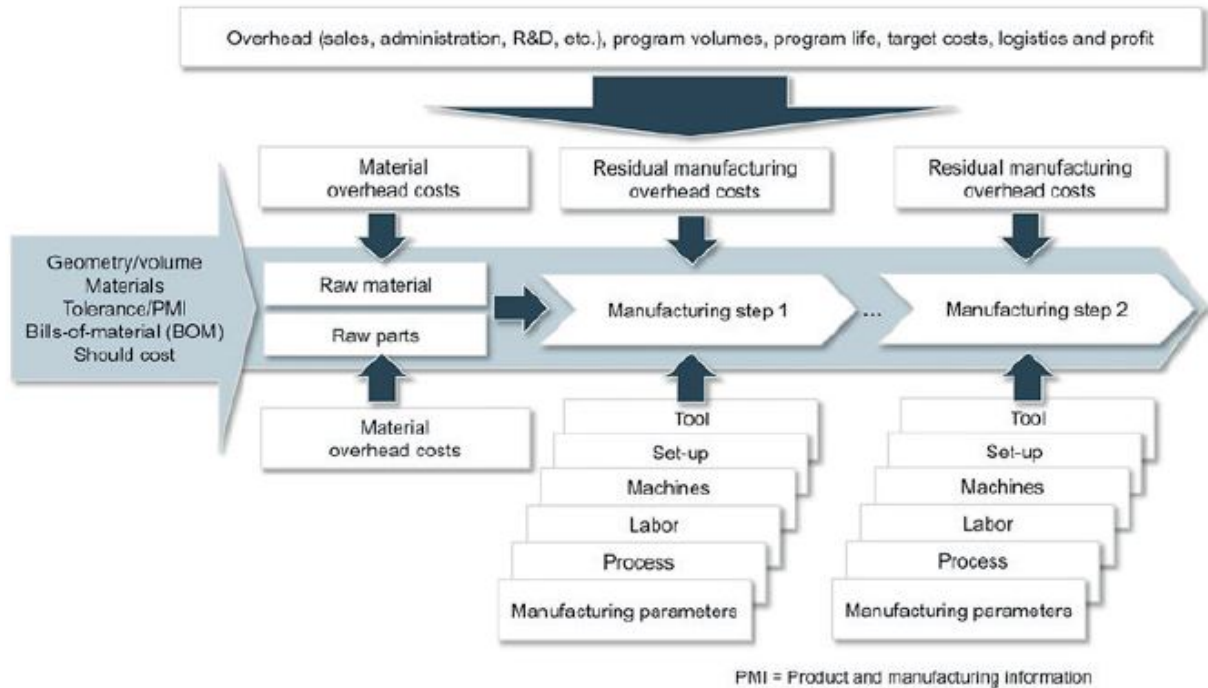


**Figure 30. Input needed for a bottom-up cost calculation in Siemens TcPCM [Source: Siemens PLM Software].**

The supply chains used for the SoA and the LOWCOST-IC approach are shown in Figure 31.

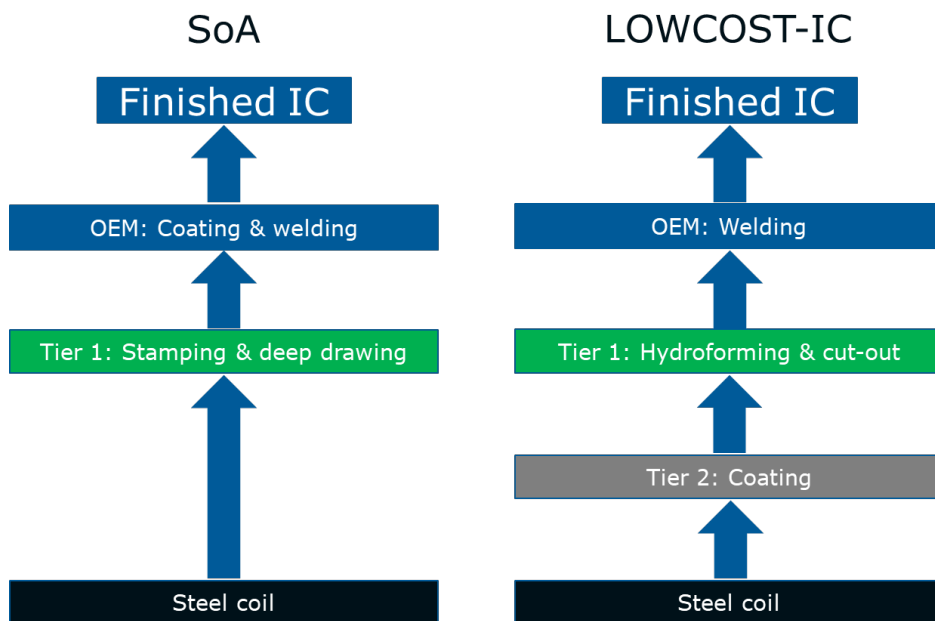


**Figure 31. Supply chain for SoA- and LOWCOST-IC routes.**



## Results

Using the methodology described above, the breakdown of cost for the SoA as well as the LOWCOST-IC production route was determined. It should be emphasized that European competition regulations laws (as well as the business interest of industrial consortium partners) do not allow the publication of in-house data of materials and process costs. Therefore, only normalized mean data can be made publicly available. In Figure 32, the mean absolute costs for the SoA and the LOWCOST-IC routes are shown (y-axis removed) and Figure 33 shows the mean relative cost shares with the SoA costs being 100 %. Please be aware that this is an optimistic high-volume scenario.

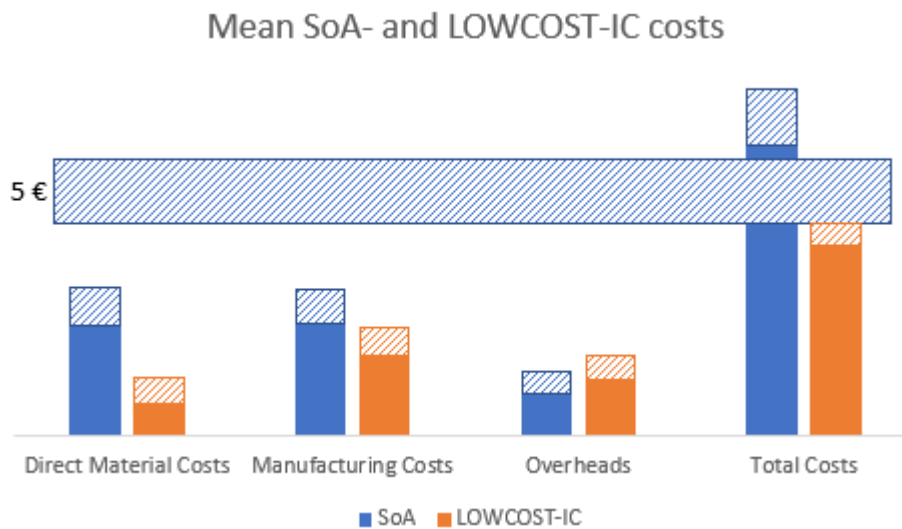


**Figure 32. Mean absolute materials-, manufacturing-, overhead- and total costs for SoA and LOWCOST-IC production routes. Please note that the SoA route is scaled to reach interconnects for 50 MW/year electricity production. The horizontal bar represent the target cost of  $5\pm 0.5$  €**

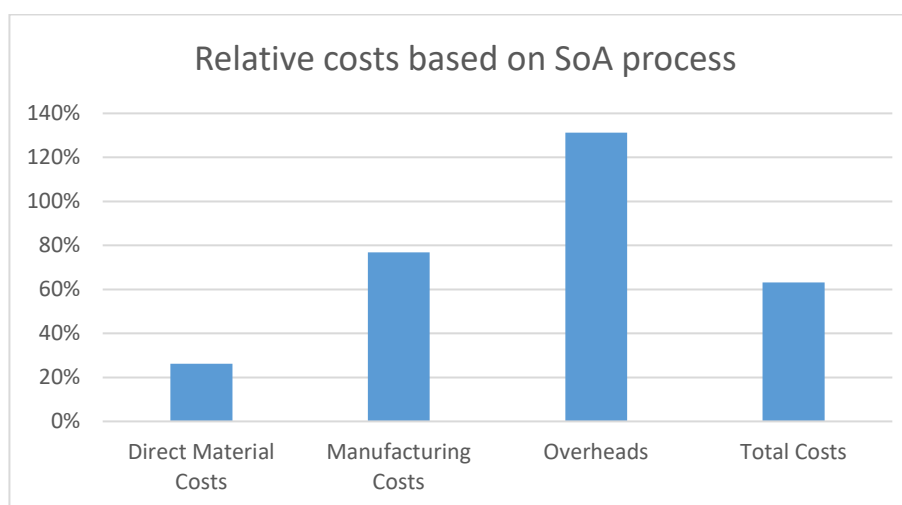


**Figure 33. Mean relative materials-, manufacturing-, overhead- and total costs compared to the SoA processing route. Please note, that the SoA route is scaled to reach interconnects for 50 MW/year electricity production.**



### Regarding Objective 2a

It was shown, that a raw material cost reduction of >80 % can be achieved for systems using Crofer 22. For systems that already make use of a standard steel, the coating cost reduction alone is not enough to achieve this level of cost reduction.

### Regarding Objective 2b

It was shown, that it is theoretically possible to reduce production costs to <5 €/interconnect for high production volumes (interconnects for 50 MW/year electricity production)

### Interpretation

**General:** When reading the data, please keep in mind that high production volume mean data is shown here, which is not applicable to all products 1:1. Nevertheless, some important trends can be derived from Figure 32 and Figure 33:

- The production costs (direct materials costs + manufacturing costs) show a big cost reduction potential.
- As shown in Figure 31, another supplier level is introduced, the overhead costs rise.
- The increase in overhead cost is much smaller than the cost-savings in production costs.

In the following, a short discussion about each category can be found.

**Direct material costs:** The biggest cost driver in direct materials costs is the interconnect steel, especially if Crofer 22 is used. The coating raw materials cost has a good cost saving potential by using cheaper/thinner coatings, but the absolute impact is not very high. For companies already using a standard steel, the main cost reduction potential thus lies in the manufacturing costs.

#### Manufacturing costs:

- For very high production volumes, costs for stamping and deep drawing are driven by tooling costs. As the tooling for hydroforming is less expensive (deep drawing needs an upper- and a lower tool, while hydroforming only needs one tool) and the tooling lasts much longer, a cost benefit can be achieved here by switching to hydroforming.
- For very high production volumes, batch-type processes like longer drying times or heat treatments are expensive. At the same time, roll-to-roll processes like printing or PVD (that can be expensive for low production volumes) become rather cheap. This is very important because these processes dominate manufacturing costs for high volume production.

**Overheads:** The changes in overheads are dominated by two factors.

- The first factor is that the supply chain structure changed. As shown in Figure 31, a tier 2 supplier for coating application is introduced in the LOWCOST-IC route before



shaping by the tier 1 supplier. This means, that another supplier puts his overheads on top of the production costs and rises overall overhead costs.

- The second factor is that overhead costs are allocated as a percentage of the production costs (= direct materials costs + manufacturing costs), meaning the **absolute** overhead costs go down as production costs go down. As the SoA costs are higher than the LOWCOST-IC costs, the value  $\frac{Costs_{LOWCOST-IC}}{Costs_{SoA}} < 1$  makes the LOWCOST-IC overheads smaller compared to the SoA overheads. Another impact of factor two is: If a product gets expensive in the first production steps and is then sold from one supplier to the next one with only very cost-effective production steps in-between, the absolute overhead costs will be higher than for products that have their expensive production steps at the OEM.

**Total costs:** The total costs show a mean cost reduction of ~35 % for high production volumes. While the direct materials costs and manufacturing costs can differ a lot from one product to another (and thus the mean cost reduction potentials can be misleading\*), the total cost reduction potential should be in this order of magnitude for most interconnects.

## T6.2 Economy of scale and T6.3 Cost benefit assessment

The economy of scale assessment and the cost benefit assessment including cost reduction potentials because of increased lifetimes are focused in the next project period and will be described in the final report.

\*For example, if a company uses expensive materials in the SoA process to then be able to dry/sinter the coating while operating the stack, the manufacturing costs could theoretically even increase, while the cost saving potential in direct material costs become even bigger. The total cost saving potential nevertheless is in the magnitude of ~35 %.

## 1.2.7 WP7 - Dissemination

### Executive summary of WP7

The overall purpose of WP7 is to increase the project impact by fostering knowledge transfer and dissemination of scientific and technological results. Furthermore, the WP will assist the commercial partners in exploiting the technical results from the project including IPR and safe data management.

For these purposes a number of plans have been generated and maintained through the project, i.e. the Plan for the Exploitation and Dissemination of Results (PEDR) and a Data Management Plan (DMP). Furthermore, a project web-site ([LOWCOST-IC.EU](http://LOWCOST-IC.EU)) has been established. This has all been done in time, although D7.5 with a small delay, which has not impacted the progress of the project.

The first workshop was planned to be held in connection with the European Fuel Cell Forum 2020 (EFCF 2020), Lucerne, Switzerland. The conference was first postponed due to the



Corona pandemic and the uncertainty on whether the conference would be held, has led to some hesitation in whether the workshop should be postponed even further. However, the EFCF 2020 conference now seems to occur also physically, and we will thus also try throw the workshop.

D7.3 is based on that we would have successful testing of the contact layers in a real stack at both SUN and SOL. However as D5.3 is delayed due to the Corona pandemic, as it will not influence any of the other project activities, we have chosen to push this well ahead.

**Table 20 Deliverables in WP7, lead partner, and delivery dates.**

Del No	Title	Lead	Original date	Delivery date/ New date
D7.1	Plan for the Exploitation and Dissemination of Results (PEDR), including a communication tool-box, finalized	DTU	M3	M3
D7.2	Project website for external communication and sharing of results among partners launched	DTU	M3	M3
D7.3	Contact four potential European suppliers (ESL ElectroScience, Schott glass, Fuel Cell Today, Kerafoil) for licensing the product	DTU	M15	M27
D7.4	Final iteration of alloy/coating combination described by a technical data sheet made available on the webpages of Aperam and Sandvik	APE	M30	M39
D7.5	Update PEDR	DTU	M12	M15

**Table 21 Milestones in WP7, lead partner, and dates reached.**

MS No	Title	Lead	Original date	Date reached/ New date
M7.1	Workshop on mechanical integrity of SOFC stacks conducted with more than 25 participants from academia and industry	DTU	M21	M24
M7.2	Workshop on corrosion and protection of interconnects conducted with more than 25 participants from academia and industry	CU	M33	M39

### T7.1 Dissemination and communication management

To promote the dissemination and communication management, a Plan for the Exploitation and Dissemination of Results (PEDR) have been established amongst the consortium partners. The PEDR was updated at M3 and M15 (D7.1 and D7.5), and will also be updated in connection with the midterm report at M20 (see Appendix A). At this stage in the project, the new products are still being evaluated and tested in the stack. Thus, no exploitations can yet be made based on the project.



Besides the scientific publications also outreach for the broader public have been undertaken, as shown in the summary in Table 22.

**Table 22 Communication activities in 2018-2019**

Date initiated	Type of activity	Title/description
Aug. 2018	Project presentation at Chalmers' website	"Fuel cell research receives Horizon 2020 funding"
Feb. 2019	Project presentation at the DTU Energy website	"Cheaper steel will make a difference for ceramic fuel cells and electrolysis cells"
Feb. 2019	Post on LinkedIn	Post of the DTU Energy project presentation "Cheaper steel will make a difference for ceramic fuel cells and electrolysis cells"
Feb. 2019	Mendeley project	<a href="https://www.mendeley.com/community/lowcost-ic/">https://www.mendeley.com/community/lowcost-ic/</a>
Mar. 2019	Launch of the LOWCOST-IC website	Project information, partner information, contact information, publications are published <a href="https://www.lowcost-ic.eu/">https://www.lowcost-ic.eu/</a>
Mar. 2019	Researchgate project	<a href="https://www.researchgate.net/project/LOWCOST-IC">https://www.researchgate.net/project/LOWCOST-IC</a>
Apr. 2019	Industrial fair: Hannover Messe	The information poster was presented (see deliverable 7.1)

### T7.2 Dissemination of results

On the intranet, a design toolbox, including templates for documents (e.g. deliverables), slides and posters have been made available to the consortium.

### T7.3 Workshop on mechanical integrity of SOFC stacks

As mentioned in the executive summary, the Corona pandemic has made it challenging to plan the first workshop on "mechanical integrity of SOFC stacks" especially with respect to meeting the target of 25 participants from academia and industry (M7.1). Currently, the plan is to throw the workshop with the consequences that this may impact the number of participants.

### T7.4 Workshops on corrosion and protection of interconnects

Not relevant to report on yet.

### T7.5 Exploitation of project results

Testing the novel contact solution in a prototype stack (WP5) will after one year constitute a new product ("contact paste for screen and inkjet printing") to serve clients (SOFC/SOFC stack



producers). DTU will contact four potential European suppliers (ESL ElectroScience, Schott glass, Fuel Cell Today, Kerafoil) for licensing the product (**D7.3**).

### **1.3 Impact**

All the impacts proposed in Section 2.1 of the DoA are still highly relevant. The interconnect steel, end plates and frames contribute significantly to the total cost of the SOC stacks<sup>3</sup>, and cost is a significant factor for the competitiveness of the SOC technologies.

The corrosion of the interconnects is also still very central for the lifetime of the SOFC stacks, both due to possible break-away corrosion for long-term exposures and thus failure of the interconnect component itself, but also because of Cr poisoning of the air electrode.

Mechanical failure of the interface between the interconnect and the air electrode is also one of the weakest points in an SOFC stack and mechanical failure is detrimental for an SOFC stack. Thus, enhancing the strength of this interface is also key for the success of particularly the SOFC technology.

The technical targets of the project all aim towards improving these overall targets.

Thus, the consortium thinks that the current targets are still highly relevant.

## **2 Update of the plan for exploitation and dissemination of result**

The plan for exploitation and dissemination is not updated at the present time. LOWCOST-IC updated the plan at M12 and due to Corona pandemic there has been a gap in conferences, presentations, fairs etc. An updated version of the PEDR has been appended this report.

## **3 Update of the data management plan**

The data management plan has been significantly updated and is now much more concrete and specific on all partner's data. An updated version of the PEDR has been appended this report.

## **4 Follow-up of recommendations and comments from previous review(s)**

**Not applicable for LOWCOST-IC**

---

<sup>3</sup> [1] S. Harboe, A. Schreiber, N. Margaritis, L. Blum, O. Guillon, N.H. Menzler, Manufacturing cost model for planar 5 kWel SOFC stacks at Forschungszentrum Jülich, Int. J. Hydrogen Energy. 45 (2020) 8015–8030. doi:10.1016/j.ijhydene.2020.01.082.



## 5 Deviations from Annex 1 and Annex 2

### 5.1 Tasks

As described in section 1.2, there have been minor deviations from the project plan resulting in minor delays of 1-3 months. This includes D2.3-D2.5, D3.4 and D3.5. These did not have any significant impact on the project progress, and is thus colored green in the above tables.

#### **Deviation of D3.1: Flow distribution for the current SUN stacks computed by the multiphysics homogenized SOC stack model and delivered to FZJ for comparison with detailed model**

The key employee at DTU carrying out D3.1 had to take leave to tend to her family. Thus D3.1 was delayed from M9 to M15.

##### **Mitigation:**

The outcome of D3.1 was to be verified with results at FZJ using on a more detailed model on the flow. Furthermore, the resulting model should be used in T3.1 for D3.2 for an initial final delivery to FZJ in M18. First of all, FZJ initiated their modelling in parallel for comparing to the results in D3.1, where some time was regained. Furthermore, this work could continue during the Corona pandemic and with the extension asked for, the deliverable D3.2 should be postponed only 3 months, providing FZJ and BOR more time to handle the production of the new interconnect design, see Figure 34 and Figure 35.

#### **Deviation of D4.2: Report on fracture energy of the cell interconnect interface with the different chemical compositions and particle sizes measured at initial operation and after 3000 hours of aging**

The company used to cut (by etching) the coated samples for mechanical testing of various interfaces after aging managed to destroy the samples *twice* (applying water to the coated surface). An alternative cutting method was then used, but precious months had been lost. This meant that DTU could not age the samples before the movement of their labs, but we managed to age the samples for 250 h (see description of T4.3, Section 2). The re-establishment of the labs was even further delayed due to the Corona pandemic and has now been almost a year (since October 2019 until August 2020). Now, the sample ageing can be initiated, but with an extensive delay.

##### **Mitigation:**

No route for mitigating this delay have been found. The results from the 250 h test were, however, very promising and toughening was observed with the aging. The preliminary results also provided the guide on the further development of the contact layers, i.e. making composite structures using, Co, Cu and Mn with a hope to achieve a good compromise between chemical stability and mechanical robustness.



### **Deviation of D5.1 and D5.2:**

The stack manufacturing in D5.1 (M6) was delayed to a minor extend at SUN but significantly at SOL (M16). This was due to production issues with the new prototype stacks, but also due to lacking production capacity at the time needed. SUN managed to catch up on their production delay, as the testing of their stack was done within time and documented in D5.2. D5.1 at SOL was however completed and is currently being tested at FZJ. Results are expected to be ready at the midterm evaluation.

### **Mitigation:**

After test, the D5.1 stack is supposed to be postmortem analysed at FZJ to reach M5.1 in T5.3. The execution of T5.3 had from the project beginning a decent time buffer built in. With this and the proposed extension due to the Corona pandemic, then we should be able to align this activity with the remaining project activities without further delays. This is illustrated in the proposed new Gantt diagram in Figure 35. When comparing to Figure 34 it is shown how the D5.1 and D5.2 can be fitted in to meet M5.1 in month 24.

D5.3 is also delayed, but this is primarily due to the Corona pandemic. Fitting in the new contact layers did however also require some extra unforeseen investigations, as it appears that the contact layers expands 400-500 % if not constrained. The point of the expansion was much needed to investigate if this could cause any problems with the current stack assembly procedures – in relation to the crystallization (solidification) of the glass ceramic-sealings etc.

### **Deviation of D5.3:**

The second set of stacks (ST2) with the two new contact layers (Mn-Co; Mn-Cu) is delayed. There are four main-reasons:

- The powders to produce a paste for CL1 were delivered with a delay of 2.5 month due to problems with procurement.
- There were safety issues processing metallic powders at SUN. A hazard assessment had to be done. Now only trained workers with protective gear are allowed to process the powders and the paste.
- The integration of the contact layers in the SUN stack design requires more tests. In the SOA stack the contact layers are already oxidised and milled to a defined height before stacking. The new contact layers would allow to get rid of the milling process, since the contact layers could adopt to the desired height by oxidising during the joining process. But the oxidation behaviour of the contact layers has to be investigated and understood, as the contact layers expands 400-500 % if not constrained. This may be problematic during the stack assembly. The oxidation kinetics and forces due to expansion is currently being investigated at DTU.
- The Corona pandemic occurred while these challenges were to be handled.

It is assumed that with a total delay of nine month, the ST2 stacks will be delivered.



**Mitigation:**

With the proposed extension due to the Corona pandemic and using a bit of buffer in the original plan (see Figure 34) we believe that we can handle these delays in the revised plan (see Figure 35). This will be sufficient for not impacting the project further.

**Deviation of D7.3**

D7.3 is based on that we would have successful testing of the contact layers in a real stack at both SUN and SOL. However, as D5.3 will be delayed due to the Corona pandemic, then we could not move forward with this task.

**Mitigation:**

As it will not influence any of the other project activities, we have chosen to push this well ahead to avoid any further delays of the deliverable.

# Gantt Diagram - original

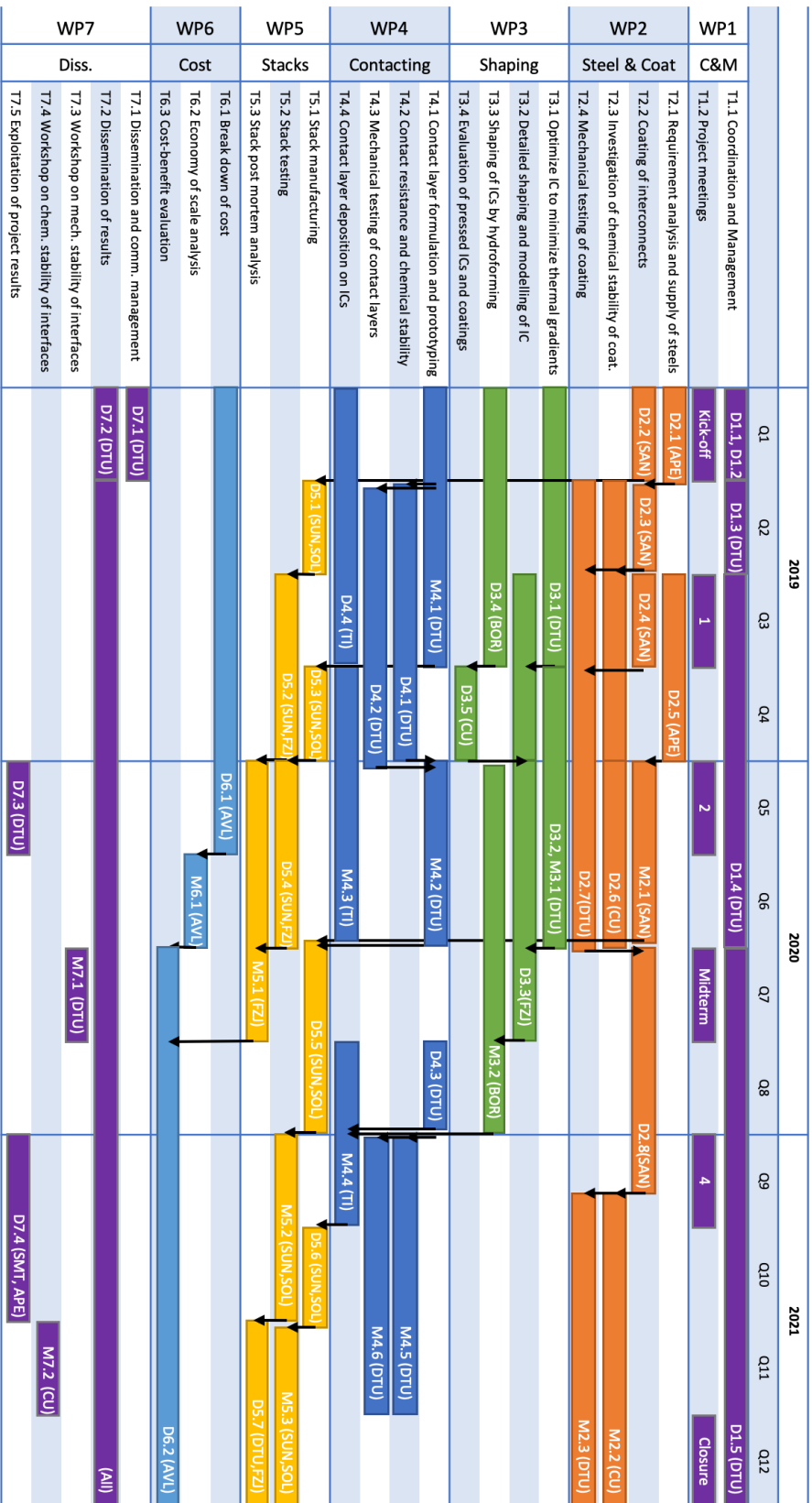


Figure 34 Original Gantt diagram

# Gantt Diagram – proposed new

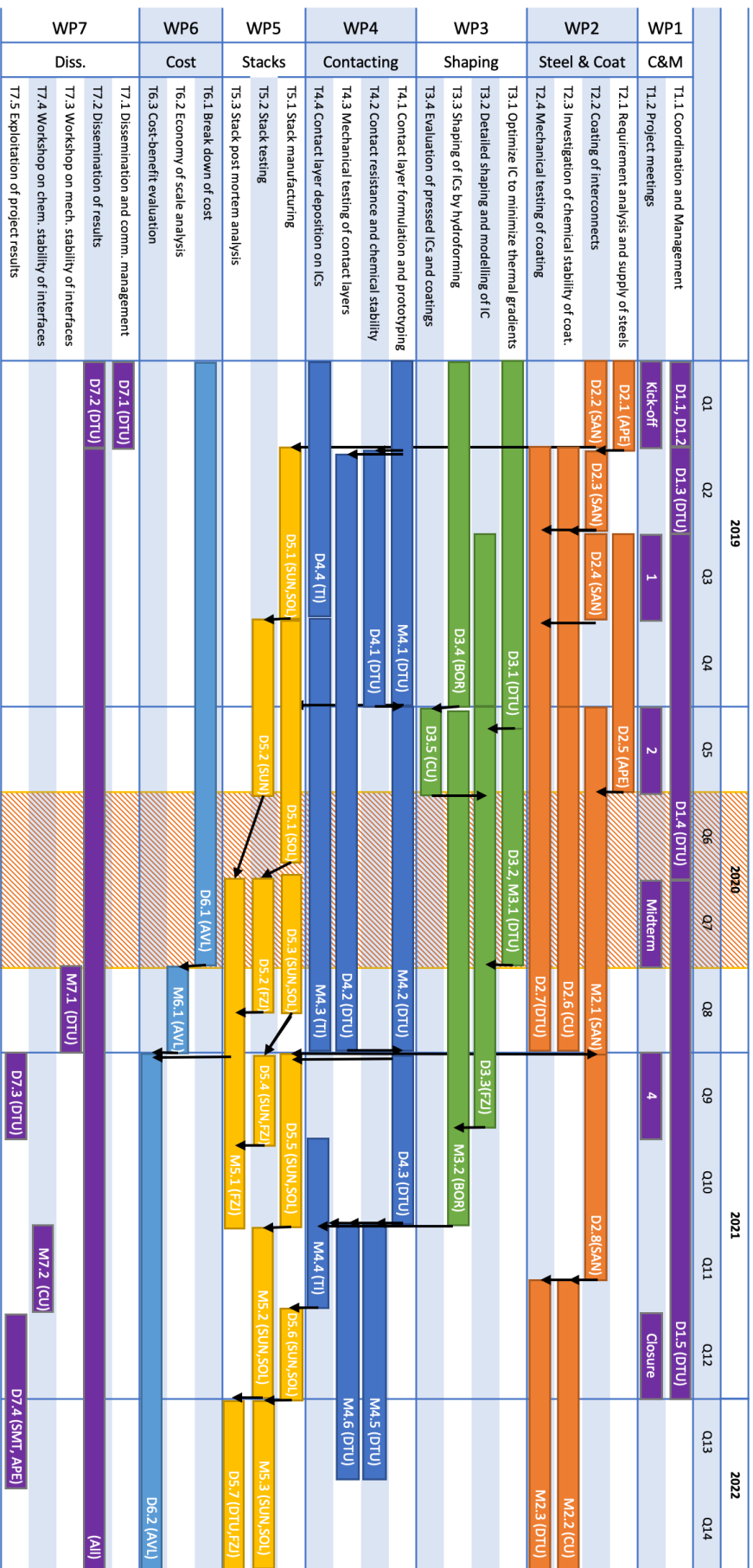


Figure 35 Proposed new Gantt diagram, with the delay of the Corona pandemic represented and updated

Table 23 Overview of total budgeted and in period (P1) spend person months at the different partners.

Partner	WP1		WP2		WP3		WP4		WP5		WP6		WP7		Total		Total % P1
	Budget	P1	Budget	P1	Budget	P1	Budget	P1	Budget	P1	Budget	P1	Budget	P1	Budget	P1	
DTU	10.5	2.8	14	7.04	12	11.61	31.5	15.98	1.5	0.11	0.5	0.17	3	1.16	73	38.87	53%
APE	0.5	0.11	1	0.9	0	0	0	0	0	0	1	0.1	1.5	0	4	1.11	28%
AVL	0.5	0	0	0	0	0	0	0	0	0	9	0.67	0.5	0	10	0.67	7%
BOR	0.5	0.19	0	0	10.5	3.34	0	0	0	0	0.5	0.07	0.5	0.15	12	3.75	31%
CU	1	0	23	15.16	3	1.84	1	0.65	0	0	0	0	2	0.51	30	18.16	61%
FZl	0.5	0.95	0	0	11	6.59	0	0	10	0	1	0	2.5	0.23	25	7.77	31%
SMT	0.5	0.3	8.5	5.9	1	0	0	0	0	0	0.5	0	0.5	0.7	11	6.9	63%
SOL	1	0.86	0	0	0	0	0	0	17	6.55	1	0.77	1	0	20	8.18	41%
SUN	1	0.5	2	0	6	0	3	1	22	5.7	3	0	1	0.5	38	7.7	20%
TI	0.5	0.06	0	0	0	0	4.5	1.63	0	0	0.5	0.06	0.5	0.06	6	1.84	31%
Total	16.5	5.8	48.5	29.0	43.5	23.38	40	19.26	50.5	12.36	17	1.84	13	3.31	229	94.95	41%



## 5.2 Use of resources

As seen in **Error! Reference source not found.** 41 % of the total project budget has been spend in the first period (P1), which is well in line with the expected spending, also taking the Corona pandemic into consideration. In some cases, highlighted with yellow in **Error! Reference source not found.**, substantially more or somewhat less have been spend. The reasons for this are:

- For DTU in WP3 the activities are coming to an end, why most of the budget have been spend already.
- For WP5 some resources have been spend, but only one of the four stacks have been produced at each of the two manufacturers, due to the reasons explained in Section 5.1. Thus, only approximately a third of the resources have been used in WP5.
- For WP6 activities have also been slightly delayed due to the Corona pandemic and the need for establishing additional NDAs, as explained in WP6, why also the majority of the work is remains to be delivered in this WP6.

### 5.2.1 Unforeseen subcontracting (if applicable)

Not applicable.

### 5.2.2 Unforeseen use of in kind contribution from third party against payment or free of charges (if applicable)

Not applicable.

## Acknowledgements



This project has received funding from the Fuel Cells and Hydrogen 2 Joint Undertaking under grant agreement No 826323. This Joint Undertaking receives support from the European Union's Horizon 2020 research and innovation programme, Hydrogen Europe and Hydrogen Europe research.